



CLARIFYING CHAOS II: BERNOULLI CHAOS, ZERO LYAPUNOV EXPONENTS AND STRANGE ATTRACTORS

RAY BROWN

*Applied Chaos Technology Corporation,
3865 Wilson Boulevard, Suite 210, Arlington, VA 22203, USA*

LEON O. CHUA

*Department of Electrical Engineering and Computer Sciences,
University of California, Berkeley, CA 94720, USA*

Received March 31, 1997; Revised November 20, 1997

In this tutorial we continue the program initiated in “Clarifying Chaos: Examples and Counter Examples” by presenting examples that answer questions in five areas:

Area 1. The Horseshoe/Bilateral Shifts/Bernoulli Systems

Since the bilateral shift (which may also be called a Bernoulli shift) plays such an important role in some definitions of chaos we show that it is possible to construct a differential equation for an electronic circuit whose time-one map,¹ is exactly a bilateral shift, in particular the baker's transformation and the cat map [Arnold & Avez, 1989]. We insist on being able to build a circuit in order to be sure that our example is not just a mathematical abstraction. Also, in this set of examples we show that we may construct chaotic maps of any desired level of complexity.

Area 2. Zero Lyapunov Exponents

Since the existence of positive Lyapunov exponents is so often used as a definition of chaos we answer the question: Are there systems with zero Lyapunov exponents which are not considered chaotic by this definition, which have outputs which are more complex than some chaotic systems? The answer is yes, and for these systems, called skew translations and compound skew translations [Cornfeld *et al.*, 1982], all the eigenvalues are 1. Further, the skew translation may be linear, having only additions (no multiplication's). Skew translations exist in any number of dimensions and can be realized as the time-one maps of an electronic circuit. Skew translations can have sensitive dependence on initial conditions and zero autocorrelations. The significance of this example is that the Lyapunov exponent is less a measure of the level of complexity than one first imagined since a higher level of complexity can be obtained from a lower exponent.

Area 3. Nonchaotic Strange Attractors

This phenomenon is reported in [Grebogi *et al.*, 1984] and further developed by other researchers. Of note in this regard is the work of Ding *et al.* [1989] where the place of this phenomenon within nonlinear dynamics is discussed. We show here that the origin of this phenomenon is found in dynamical systems having orbits with low correlations regardless of their Lyapunov exponents. We present examples of skew translations having zero autocorrelations

¹The terms “time-one map” and “Poincaré map” are, today, used interchangeably even within mathematical circles. While some differences in their precise definitions do exist, these differences do not affect the present-day usage of these terms.

and zero Lyapunov exponents that can be used to generate nonchaotic strange attractors. Further, we show that only minimal level of complexity is needed to obtain nonchaotic strange attractors by using a group rotation to produce one. The inverse of this idea is the chaotic nonstrange attractor which is also presented.

Area 4. Nonlinearity

Since nonlinearities are usually considered a key ingredient of chaotic dynamical systems we present examples to show that there are at least four distinct types of nonlinearities in ODEs leading to varying levels of chaos. All example ODEs have closed-form solutions in terms of elementary functions and thus give us direct insight into how the type of nonlinearity appears in the ODE and is manifested in its solution.

Area 5. Relationship of Dissipation, Noninvertibility, Nonorientibility and Chaos

There are many misconceptions about how these properties, especially dissipation, may contribute to chaos. We show that these properties are independent of chaos.

The overriding conclusion of this set of examples is that what we have traditionally called chaos is so varied in its level of complexity that it is almost a meaningless term when used by itself. In particular, the term “level of complexity” must be appealed to so often in order to clarify the varying degrees of chaos that the two terms “chaos” and “level of complexity” seem inseparable in any practical discussion of chaos. The key issue that gives rise to this confusion about the level of complexity of a chaotic dynamical system is its long- and short-term predictability. Chaotic dynamical systems may be quite predictable over very long but finite time scales, but unpredictable in infinite time. The need to consider system behavior over long, finite time scales is a practical matter and leads to the conclusion that the study of chaos must be concerned with both asymptotic and long, but finite, time dynamics.

1. Introduction

Poincaré–Birkhoff–Smale chaos, a term coined by J. Marsden, designates the family of chaotic dynamical systems for which the system is conjugate to a root of a shift² on a subset of its domain. This situation is often described by saying that the system has a horseshoe. While this definition cannot yet be proven to encompass all chaotic dynamical systems, it does represent a significant, if not the most significant, class of chaotic dynamical systems. Extensive literature exists which is devoted to showing systems which are chaotic by proving the presence of a horseshoe. There are, however, two quirks in this definition: (1) The horseshoe may exist on a set of measure zero; and (2) The system may be conjugate to such a small root of the shift that it has a very low order of complexity. This low level of complexity may result in the system having such a predictable nature over long but finite-time scales that the term “chaos” is misleading.

In Sec. 2, in order to convey an intuitive grasp of the meaning of the horseshoe in a useful formula, we construct an example of an ODE whose time-one map is exactly a horseshoe, not a root. Also, we show how routine it is to construct examples which illustrate how systems can be conjugate to a shift on a set of measure zero. Further, we examine numerous methods of altering a Bernoulli system so that enough of its level of complexity is retained to call the resulting system chaotic. This line of thought is motivated by the proof of Kalikow that one Bernoulli system may be used to modify another in such a way that the resulting system is a Kolomogrov system which is not Bernoulli [Walters, 1982]. In our recent paper *From Almost Periodic to Chaotic: The Fundamental Map* we demonstrated just how extraordinarily such modified Bernoulli systems may behave.

In Sec. 3 we construct examples of systems which meet some of the criteria of chaos, but which

²A mapping f is a root of a shift, S , when, for some positive integer n , $f^n(x) = S(x)$. For example, $x \rightarrow 2x \bmod(1)$ is a root of $x \rightarrow 4x \bmod(1)$.

have zero Lyapunov exponents. These examples demonstrate the limitations of the most popular definition of chaos, positive Lyapunov exponents, and raise the question of how is a system's *level of complexity*, in a practical sense, best measured in dynamical systems.

In Sec. 4 we demonstrate the basic construction of nonchaotic strange attractors and show how they may arise from even linear skew translations on the two-dimensional torus.

In Sec. 5 we present examples to illustrate how four different features of dynamical systems may be modified to make it nonlinear. The point of this set of examples is to expand our insight into two-dimensional systems in a way not afforded by the traditional analysis of the Poincaré–Bendixson theory.

In Sec. 6 we clarify the relationships between dissipation, noninvertibility, nonorientation preserving, and chaos.

In Sec. 7, we summarize this paper and also summarize the combined results of our first paper and this paper.

In the following discussions we will use some abbreviations introduced in the first tutorial [Brown & Chua, 1996a], and include several more that will be used throughout this paper:

Abbreviations

Sensitive dependence on initial conditions (SD), Zero Autocorrelation (ZA), Zero Lyapunov exponent (LZ), Positive Lyapunov Exponent (LP), Zero Entropy (ZE), Strange Attractor (SA), Ergodic (E), Weak Mixing (WX), Strong Mixing (SX), Kolmogorov (K), Bernoulli (B).

The formal definitions of the last five abbreviations are from ergodic theory and can be found in [Walters, 1982]. In short, they are measures of how well a transformation mixes up its domain when iterated over an infinite time span. Ergodic is the lowest form of mixing and Bernoulli the highest. Dynamical systems that have one of these forms of mixing have some level of complexity. Chaos is usually associated with B in some way.

Algorithmic Complexity and Level of Complexity

The concept of algorithmic complexity developed by Chaitin, Kolmogorov, and others is used to distinguish two levels of complexity. In reference to infinite sequences of integers, a sequence has positive

algorithmic complexity when the number of binary bits required to code the shortest computer program needed to produce the sequence is just about the same length as the number of binary bits required to write the sequence out explicitly. For infinite sequences, this number is defined in such a way that either it is positive or zero. A sequence of positive algorithmic complexity is, “essentially”, random. Zero algorithmic complexity thus denotes sequences that are less than random. This encompasses all sequences which can be described by a finite algorithm. The square root of a prime number is such a sequence, as is the number π , and all other physical constants. This notion of complexity is too limiting for our use and so we introduce the notion of a *level of complexity* of a sequence. Entropy is a measure of a level of complexity, as is autocorrelation, and information. The Lyapunov exponent is a measure of a level of complexity as well. In the study of chaos, various researchers appeal to these measurements to characterize dynamical systems that have a degree of unpredictability or intractability. The complexity spectrum is a term introduced in [Brown & Chua, 1997] as a means of talking about all of these measurements of a dynamical systems collectively. No formal definition has yet been formulated.

2. Bernoulli Chaos

In our previous tutorial we presented numerous examples and counter-examples designed to sharpen our thinking about the definition of chaos. That paper served to show that the manifestations of chaos are varied and difficult to summarize in a single definition. In order to better understand the variety of ways in which chaos can arise, we begin with the Bernoulli systems, possibly the highest form of chaos, and carry out a program of systematic “dilution” of this form of chaos until chaos disappears altogether. The methods that we use to modify a Bernoulli system reveal how chaotic systems may arise. The most important motivating example is that of Kalikow of a Kolmogorov automorphism which is constructed by using one Bernoulli system to modify another in such a way that the resulting system is not Bernoulli, but is Bernoulli on a set of measure zero.

Once we have hit upon the idea of modifying Bernoulli systems as a means of creating chaos we may take off with this idea in all directions.

Among the ways to modify a Bernoulli system are:

- (1) Form a cross-product between a Bernoulli and nonBernoulli;
- (2) Form a partial product of Bernoulli with any other map, including Bernoulli (K -automorphisms);
- (3) Compose Bernoulli and nonBernoulli;
- (4) Form a function of a component of a Bernoulli (logistic map);
- (5) Form the weighted average of a Bernoulli and nonBernoulli system (the fundamental map) [Brown & Chua, 1996].

This list is incomplete. The different ways a Bernoulli system may be modified to make a chaotic system are likely to be so numerous and varied that no single characterization would be possible.

2.1. *The Bernoulli map*

In our paper on the fundamental map [Brown & Chua, 1996b] we showed how to construct a function of a two-sided Bernoulli map. We repeat a portion of that construction as background to our derivation of the sequence of iterates of the cat map.

Before we repeat that construction we note that the map that is most easily proven to be a two-sided Bernoulli shift is the baker's transformation, [Arnold & Avez, 1968]. The most familiar formulation of this map is

$$\begin{pmatrix} x \\ y \end{pmatrix} \rightarrow \begin{pmatrix} 2x \\ y/2 \end{pmatrix} \text{mod}(1) \quad (1)$$

for $0 \leq x \leq 1/2$ and

$$\begin{pmatrix} x \\ y \end{pmatrix} \rightarrow \begin{pmatrix} 2x \\ (y+1)/2 \end{pmatrix} \text{mod}(1) \quad (2)$$

for $1/2 \leq x \leq 1$. This map formulation can be greatly simplified by the use of the notation $[x]$ which denotes the integer part of x . In this notation we have:

$$\begin{pmatrix} x \\ y \end{pmatrix} \rightarrow \begin{pmatrix} 2x \\ ([2x] + y)/2 \end{pmatrix} \text{mod}(1). \quad (3)$$

If we use $\{x\}$ for the fractional part of x this simplifies to

$$\begin{pmatrix} x \\ y \end{pmatrix} \rightarrow \begin{pmatrix} \{2x\} \\ ([2x] + y)/2 \end{pmatrix}. \quad (4)$$

In this form, a closed-form solution for the n th term of this sequence is (note that this solution is not in terms of elementary functions):

$$\begin{pmatrix} \{2^n x\} \\ ([2^n x] + y)/2^n \end{pmatrix}. \quad (5)$$

Note that everything we have said about this map carries over to the case where 2 is replaced by any positive integer k . Thus

$$\begin{pmatrix} \{k^n x\} \\ ([k^n x] + y)/k^n \end{pmatrix} \quad (6)$$

is a formula for the n th iterate of a bi-lateral shift on k symbols. While this sequence can be made the time-one map of an ODE representing an electronic circuit by our usual methods [Brown & Chua, 1992], we will direct our attention to the cat map instead. This is because the cat map is also a Bernoulli shift [Katznelson, 1971] and its solution can be expressed in terms of the elementary functions. Hence we will use the cat map as our basic example of a Bernoulli map, although the proof in case of the baker's transformation is easier to see [Arnold & Avez, 1968, Appendix 7].

As in [Brown & Chua, 1996b], let

$$\begin{pmatrix} u \\ v \\ w \\ z \end{pmatrix} = \begin{pmatrix} \cos(x) \\ \sin(x) \\ \cos(y) \\ \sin(y) \end{pmatrix}. \quad (7)$$

By direct substitution, application of the double-angle formulas for the sine and cosine, and simplification, we get the following four-dimensional system, T , on a two-dimensional space:

$$T \begin{pmatrix} u \\ v \\ w \\ z \end{pmatrix} = \begin{pmatrix} 0 & 0 & (u^2 - v^2) & -2uv \\ 0 & 0 & 2uv & (u^2 - v^2) \\ w & -z & 0 & 0 \\ z & w & 0 & 0 \end{pmatrix} \times \begin{pmatrix} u \\ v \\ w \\ z \end{pmatrix}. \quad (8)$$

In complex coordinates this map is given by:

$$T \begin{pmatrix} w \\ z \end{pmatrix} = \begin{pmatrix} w^2 z \\ wz \end{pmatrix} \quad (9)$$

where $|w| = |z| = 1$. A simple computation shows that this mapping is 1-1, in particular:

$$T^{-1} \begin{pmatrix} w \\ z \end{pmatrix} = \begin{pmatrix} w\bar{z} \\ z^2\bar{w} \end{pmatrix}. \quad (10)$$

We now write the sequence of iterates of the cat map in closed form in terms of elementary functions. The key to doing this is the derivation of an expression for the n th power of the matrix used in the definition of the cat map. Let

$$A = \begin{pmatrix} 2 & 1 \\ 1 & 1 \end{pmatrix} \quad (11)$$

then

$$A^n = \frac{1}{(1-\lambda^2)\lambda^{n-1}} \begin{pmatrix} \lambda^{2n}(1-\lambda) + (2-\lambda) & 1-\lambda^{2n} \\ 1-\lambda^{2n} & (\lambda^{2n}(1-\lambda) + (1-2\lambda))/\lambda \end{pmatrix} \quad (12)$$

where $\lambda = 0.5(3 + \sqrt{5})$, which is the largest eigenvalue of the matrix A . Using this we may write the n th term in the sequence of iterates of this map. For notational convenience let

$$\begin{pmatrix} a_n & b_n \\ c_n & d_n \end{pmatrix} = \frac{1}{(1-\lambda^2)\lambda^{n-1}} \begin{pmatrix} \lambda^{2n}(1-\lambda) + (2-\lambda) & 1-\lambda^{2n} \\ 1-\lambda^{2n} & (\lambda^{2n}(1-\lambda) + (1-2\lambda))/\lambda \end{pmatrix}$$

then

$$\begin{pmatrix} u_n \\ v_n \\ w_n \\ z_n \end{pmatrix} = \begin{pmatrix} \cos(a_n\phi_0 + b_n\theta_0) \\ \sin(a_n\phi_0 + b_n\theta_0) \\ \cos(c_n\phi_0 + d_n\theta_0) \\ \sin(c_n\phi_0 + d_n\theta_0) \end{pmatrix}. \quad (13)$$

Note that $b_n = c_n$.

This is the closed-form solution we seek for the chaotic mapping on the torus. By taking arctangents we obtain the Bernoulli iterates in terms of the elementary functions.

What we have done, as in our example of the logistic map, is not very complex. To obtain the solutions we sought, we needed only to find a method of getting around the use of the modulo(1) operation. The basic technique of doing this was explained in [Brown & Chua, 1996a]. The key idea to note, periodic functions perform the same operation as the modulo(1) function.

2.2. The Bernoulli map as a Poincaré map

By employing a two-phase gate we may construct the equations of a nonautonomous ODE whose Poincaré map is the Bernoulli map. This technique is explained in [Brown & Chua, 1993]. We have the following equation for which the Bernoulli map is the Poincaré map:

$$\begin{pmatrix} \dot{w} \\ \dot{z} \end{pmatrix} = \begin{pmatrix} (1-s(t))w \log(z) \\ s(t)z \log(w) \end{pmatrix} \quad (14)$$

where $s(t) = 0.5(1 + \text{sgn} \sin(\omega t))$. Initial conditions must be taken to have absolute value 1.

The Bernoulli map can be written, as this equation suggests, as a composition of two maps:

$$T_1 \begin{pmatrix} w \\ z \end{pmatrix} = \begin{pmatrix} w \\ zw \end{pmatrix} \quad (15)$$

$$T_2 \begin{pmatrix} w \\ z \end{pmatrix} = \begin{pmatrix} wz \\ z \end{pmatrix} \quad (16)$$

which are time-one maps for autonomous ODEs. The Bernoulli map is $T_2 \circ T_1$. The component maps arise as time-one maps of the solutions of two systems of ODEs. The solutions are as follows:

$$\begin{pmatrix} w_1(t) \\ z_1(t) \end{pmatrix} = \begin{pmatrix} w_0 \\ z_0 w_0^t \end{pmatrix} \quad (17)$$

$$\begin{pmatrix} w_2(t) \\ z_2(t) \end{pmatrix} = \begin{pmatrix} w_0 z_0^t \\ z_0 \end{pmatrix} \quad (18)$$

which are the solutions of the separate component ODEs corresponding to the two phases of the function $s(t)$.

These equations are presented in complex form for convenience. The complex representation is not essential and no complex variable theory has been used in our analysis.

Now that we have a Bernoulli mapping in an algebraic formula we proceed to utilize this map to

construct examples of chaos which are less than Bernoulli.

2.3. *Cross products with Bernoulli systems*

The simplest way to obtain a map which is Bernoulli on a set of measure zero is to have at least one component of a cross product to be Bernoulli, and one that is not Bernoulli. Let,

$$T \begin{pmatrix} u \\ v \\ w \end{pmatrix} = \begin{pmatrix} u^2v \\ uv \\ aw \end{pmatrix} \quad (19)$$

where the first two components are restricted to have modulus 1. If we choose $w_0 = 1$, and $0 < a < 1$, we form orbits for which the third coordinate converges to 0 but the first two are Bernoulli. By construction, T is not Bernoulli but is Bernoulli on a set of measure zero. Further, the points of the first two components form a two-dimensional attractor which is Bernoulli.

The three-dimensional image of the orbits of the map defined by Eq. (19) is shown in Fig. 1. As

seen there, the orbit converges to a two-dimensional square which is the attractor. Another way of looking at this figure is to think of the third coordinate as a time parameter. With this point of view, the time evolution of the Bernoulli map is portrayed by the third dimension. The uniformity of the points that lie above the attractor portray the randomness of the orbit. If the points that lie above the attractor formed a pattern, we would know that the Bernoulli system determined by the first two coordinates is less than random. This brings us to Fig. 2, another Bernoulli map. In this case, instead of our map being the analog of the one-dimensional map $2x \bmod(1)$, it is the analog of $1.032x \bmod(1)$. This map thus has a positive Lyapunov exponent, ≈ 0.032 , and is the root of a shift, a horseshoe. However, as seen in Fig. 2, it is less than random, having distinctive pattern features in its orbit. Figure 2 shows that having a positive Lyapunov exponent does not mean that there is a high degree of randomness, or chaos in the map, even though, by any definition, it is chaotic.

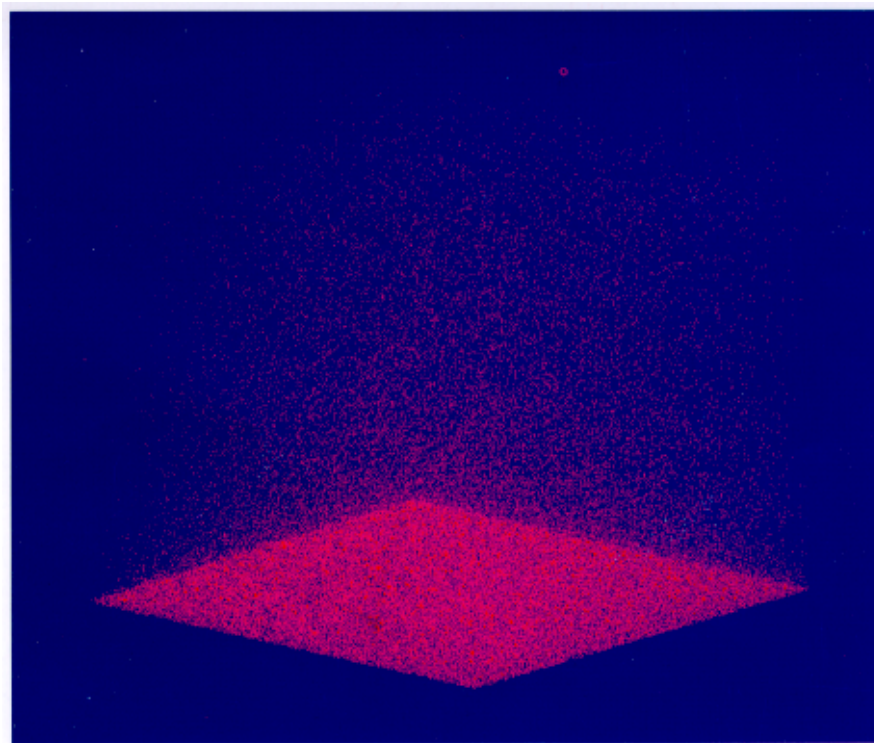


Fig. 1. In Fig. 1 we have made the domain, a square, of the cat map an attractor. The result is that, when the initial condition has a nonzero z value the orbit is attracted to a square in the $x - y$ plane. The effect is reminiscent of mist rising from a body of water.

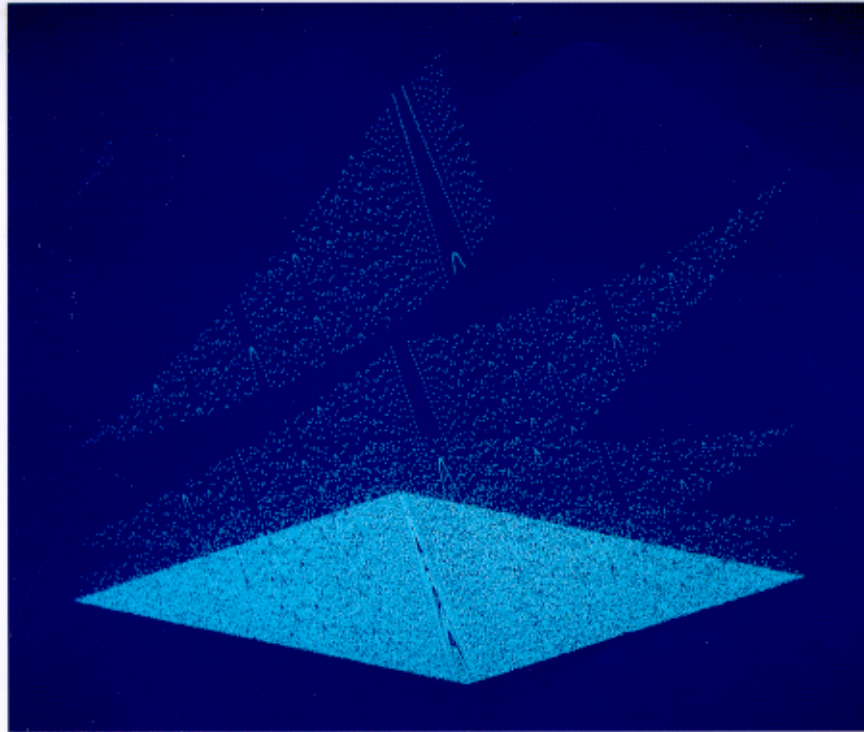


Fig. 2. In Fig. 2 we modified the cat map to have a Lyapunov exponent of ≈ 0.039 . The figure format is exactly the same as Fig. 1. The result is the development of nonchaotic graphical features. By making the range of the modified cat map an attractor, this breakdown in the level of complexity is clearly visible in the part of the orbit above the attractor.

2.4. K -automorphisms

Following an example of Kalikow from [Walters, 1982] we construct (without proof) a map which is a K -automorphism:

$$K \begin{pmatrix} u \\ v \\ w \\ z \end{pmatrix} = \begin{pmatrix} u^2v \\ uv \\ \text{sg}(u)(w^2z) + (1 - \text{sg}(u))(w\bar{z}) \\ \text{sg}(u)(wz) + (1 - \text{sg}(u))(z^2\bar{w}) \end{pmatrix} \quad (20)$$

where $\text{sg}(u) = 0.5(1 + \text{sgn}(0.5 + \cos(\arg(u)))$. We note that K has a set of measure zero on which it is Bernoulli in analogy with the horseshoe of Smale. The construction is not a direct product, so we call it a partial product.

Figure 3 is a three-dimensional illustration of a modification of this map. The modification is to the first component where, for convenience, we have used the logistic map as a one-dimensional source of chaos to be used to switch between the cat map and its inverse. The exact equation for Fig. 3 is as

follows:

$$K \begin{pmatrix} u \\ w \\ z \end{pmatrix} = \begin{pmatrix} 4u(1-u) \\ \text{sg}(u)(2w+z) + (1 - \text{sg}(u))(w-z) \\ \text{sg}(u)(w+z) + (1 - \text{sg}(u))(2z-w) \end{pmatrix} \times \text{mod}(1) \quad (21)$$

where $\text{sg}(u) = 0.5(1 + \text{sgn}(0.5 - u))$.

This example captures the essence of Eq. (21) while being simpler to implement on a computer. In the vertical dimension, K is just the logistic map. In the z, w dimension K alternates between the cat map and its inverse. The Lyapunov exponent in the z, w dimensions is the same as the cat map. However, the level of complexity of the orbit that cat map contributes is being constantly reversed by its inverse. The possibility of global chaos that comes from the cat map must always be compromised by the inverse, thus leaving only local, finite excursions of chaos that come from long runs by the logistic map having a value above 0.5. Thus the chaos of this map is actually being imparted by the logistic map. We will see in Sec. 3 that it is possible to construct an example of a three-dimensional map from Eq. (21) where we replace the first two components

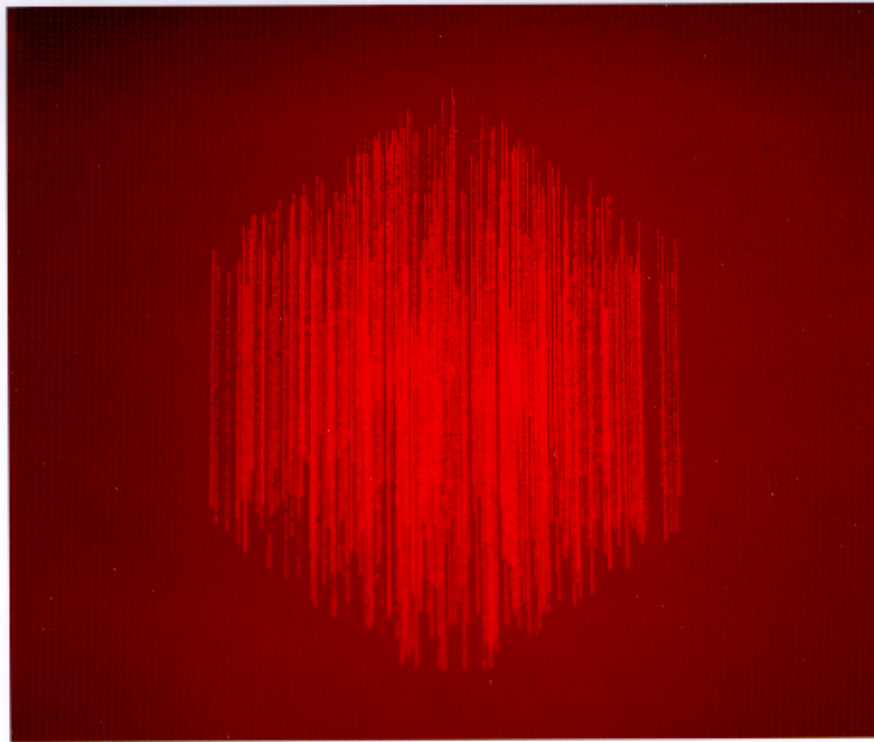


Fig. 3. The orbit of the K map of Eq. (21) is presented with the same format as Figs. 1 and 2. While there are no orderly geometric features present as there are in Fig. 2, the orbit is clearly different from the cat map.

with a map which has a LZ, ZA, E, and hence it looks “random.”

2.5. *Other partial products*

The following example is neither Bernoulli, K , nor almost periodic, but has a set of measure zero on which it is Bernoulli:

$$K \begin{pmatrix} u \\ v \\ w \\ z \end{pmatrix} = \begin{pmatrix} u^2v \\ uv \\ \text{sg}(u)(w^2z) + (1 - \text{sg}(u))(aw) \\ \text{sg}(u)(wz) + (1 - \text{sg}(u))(bz) \end{pmatrix} \quad (22)$$

since the third and fourth components of the map alternate “randomly” between Bernoulli and are almost periodic.

We note that by replacing the function $\text{sgn}(u)$, which occurs in the definition of the function $\text{sg}(u)$, in the above equations with a sigmoid function we make all examples infinitely differentiable.

2.6. *Gated compositions with Bernoulli systems*

We have shown how to use a two-phased gate to

construct Poincaré maps from time-one maps of autonomous ODEs [Brown & Chua, 1993]. In those constructions we choose each phase of the gate to have equal time. Using a gate which does not have equal time gives us another construction. We explain this construction in two steps. First we describe the gate:

$$s_1(t) = 1 \quad \text{for } 0 \leq t < 1 \quad (23)$$

$$s_1(t) = 0 \quad \text{for } 1 \leq t < 3 \quad (24)$$

$$s_1(t+3) = s_1(t) \quad (25)$$

$$s_2(t) = 1 - s_1(t) \quad (26)$$

Note that $s_2(t)$ is nonzero twice as long as $s_1(t)$. Using this gate we define a general nonautonomous ODE:

$$\dot{x} = s_1(t)F_1(x) + s_2(t)F_2(x). \quad (27)$$

The Poincaré map determined by sampling the map at times $t = 1, 2, 3, \dots$, results in one point of the orbit being determined by $\dot{x} = F_1(x)$ and the next two points being determined by $\dot{x} = F_2(x)$, then back to the F_1 equation. The Poincaré map is not simply the composition of the maps determined by F_1 and F_2 because we must actually get one point

of the orbit from the F_1 equation and then get *two* points from the F_2 equation. A composition would omit the intermediate points, only recording the result of applying the F_1 equation and then the F_2 equation to the initial point. The presence of these intermediate points being included in the orbit is significant in that they alter the geometry and the level of complexity of the orbit.

The time difference between the two phases may be as long as we desire. In our example this ratio is 1:2. The greater the ratio between the phases the greater the difference in the contribution to the orbit by the two phases. In this way, we may combine a Bernoulli phase with an almost-periodic phase in such ratios (say, 1:1000000) that the Bernoulli contribution is as thin as we please and the resulting orbit must still be chaotic. This technique shows how to include a Bernoulli system at any desired level we choose to construct a chaotic orbit whose chaotic features are as “thin” as we choose. The mechanism illustrated by this example could easily be reflected in a real-world system in which complex forces alternated with periodic forces to shape some geological feature or biological feature of a life form.

Another technique we may use is to construct the time one-half map, i.e. sample the orbit at intervals of $t = 1/2$. In this way we get two Bernoulli points followed by four almost-periodic points. Doing this amounts to refining the gates into four phases, each gate being decomposed into two phases over its nonzero range. The technique of gate refinement corresponds to the mathematical technique of refining a partition of the real line, so often used in measure theory and ergodic theory. Using the refinement method we can now construct the ODE which is a gated composition of Bernoulli and almost periodic. After all the simplifications we get a three-phased gate as follows:

$$s_1(t) = 1 \text{ for } 0 \leq t < 1 \quad (28)$$

$$s_1(t) = 0 \text{ for } 1 \leq t < 6 \quad (29)$$

$$s_2(t) = 0 \text{ for } 0 \leq t < 1 \quad (30)$$

$$s_2(t) = 1 \text{ for } 1 \leq t < 2 \quad (31)$$

$$s_2(t) = 0 \text{ for } 2 \leq t < 6 \quad (32)$$

$$s_3(t) = 0 \text{ for } 0 \leq t < 2 \quad (33)$$

$$s_3(t) = 1 \text{ for } 2 \leq t < 6 \quad (34)$$

We extend the functions to be periodic of period 6. Now we define our gated-circuit equation in complex variable notation:

$$\begin{pmatrix} \dot{w} \\ \dot{z} \end{pmatrix} = \begin{pmatrix} s_1(t)w \log(z) + s_3(t)z \\ s_2(t)z \log(w) - \lambda^2 s_3(t)w \end{pmatrix}. \quad (35)$$

By altering the ratios of the gate we obtain any level of chaos desired.

Functions of Bernoulli Systems

In [Brown & Chua, 1996a], we showed how to compose periodic functions with exponential functions to get closed-form solutions to chaotic equations. The basic process can be extended to Bernoulli systems.

Weighted Averages of Bernoulli and NonBernoulli Systems

In [Brown & Chua, 1996b], we illustrate how to combine Bernoulli with almost periodic to obtain a wide range of chaotic maps.

2.7. Chaotic systems from Bernoulli time

Since exponential stretching can generate chaos, any system that “circulates” through a region of exponential stretching an infinite number of times that is not offset by a equal amount of contracting may produce chaos. (Even if it circulates through an equal amount of contracting, it may still produce chaos.) Typically, circulation through a region of exponential stretching will depend on the initial conditions.

Bernoulli systems are an easy source of exponential stretching and, as we have shown earlier, may be decomposed into two maps which are each *nonexponentially* stretching. Hence we need only circulate through nonexponentially-stretching regions in some manner to generate chaos. An important question is whether we may circulate through a stretching region in an almost periodic manner and generate chaos. The answer is yes, since the unstable manifold of the Bernoulli system on the torus, the cat map, winds through the torus in an almost periodic manner. If this manifold were the orbit of a point moving with constant velocity the result would be almost periodic motion. This

comment leads to our next means of creating chaos from Bernoulli systems:

- (6) Starting with a continuous-time system on a bounded manifold which is almost periodic and whose orbits have infinite arc length, we change the time parameter from t to $\exp(t)$.

Having connected orbits of infinite arc length assures that the new system is invertible. If the arc length is finite, such as a circle, then the resulting system can be noninvertible. (For example, $x = \cos(\exp(t))$, $y = \sin(\exp(t))$.) By using the torus instead of a circle we have room to maneuver out of the way of previous points in the orbit. In particular, starting with any orbit on the torus inclined at an irrational angle from the vertical we obtain an orbit of infinite arc length on which we may move forward in exponential time to create chaos. This amounts to wrapping an orbit of $\dot{x} = x$, $\dot{y} = y$ around the torus inclined at an irrational angle. Generalizing this concept we have the following method of generating chaos from Bernoulli systems:

- (7) Given any bounded manifold on which there is a vector field with integral curves having infinite arc length, we may change the time parameter to exponential time and obtain a chaotic system. It is only necessary to change the time to a^t for $a > 1$ to obtain chaos.

As a variation on this idea we have the following method of generating chaos from Bernoulli systems:

- (8) Given any sequence, we may intersperse an infinite number of points from a Bernoulli sequence by any rule and the resulting sequence becomes chaotic.

2.8. Bernoulli space-time

As we have noted, we may make almost periodic systems chaotic by changing the time scale. In general, a time scale which is accelerating cannot be distinguished from a uniform time scale in which spatial coordinates are accelerating. Thus, nonuniform Space-Time acceleration can give rise to chaos. Of course, this is “relative” to an imagined observer moving in a nonaccelerating frame. The nonuniform acceleration we are most interested in is the sort in which an object has some magnitude which is accelerating and decelerating, since no magnitude

can increase indefinitely. An example is a planetary system consisting of three planets grouped as a unit (think of the earth having two large moons), orbiting around a star. Their mutual gravitational attractions can cause their orbits to be chaotic. The result is that there is no uniform time scale, since on each planet the sun rises at a different time during each revolution. The time scale is Bernoulli, and these life forms, if they could exist, live in Bernoulli Space-Time.

3. Complex Dynamics from Maps with Zero Lyapunov Exponents (LZ)

We now present examples to show that systems with zero Lyapunov exponents can produce a level of unpredictability greater than some chaotic systems.

The rationale for these examples is a theorem of Weyl [1916], and our observations in [Brown & Chua, 1996a] that the sequence $\sin(n^2)$ is uncorrelated and uniform. The example to be given is well known to ergodic theory but less known in the general scientific community. Also, we show how to make this map a Poincaré map for an electronic circuit. The map is:

$$T \begin{pmatrix} x \\ y \end{pmatrix} = \begin{pmatrix} x + y \\ y + \tau \end{pmatrix} \text{mod}(1) \quad (36)$$

If τ is irrational, this map is ergodic(E). Further, it is not a simple rotation, hence its orbits are not almost periodic. The eigenvalues are 1, 1, hence the Lyapunov exponent (LZ) is 0. Further, it has zero entropy (ZE), see [Peterson, 1983] for all facts. This is a two-dimensional example of what is called in ergodic theory a *skew translation*. In complex coordinates it can be expressed as

$$T \begin{pmatrix} w \\ z \end{pmatrix} = \begin{pmatrix} wz \\ az \end{pmatrix} \quad (37)$$

where $|a| = |w| = |z| = 1$. We recall that a twist on the torus is written as

$$T \begin{pmatrix} w \\ z \end{pmatrix} = \begin{pmatrix} wz \\ z \end{pmatrix} \quad (38)$$

and so if $a = 1$ the twist and the skew translation are the same. Also, recall that a Bernoulli mapping on the torus is given by the composition of

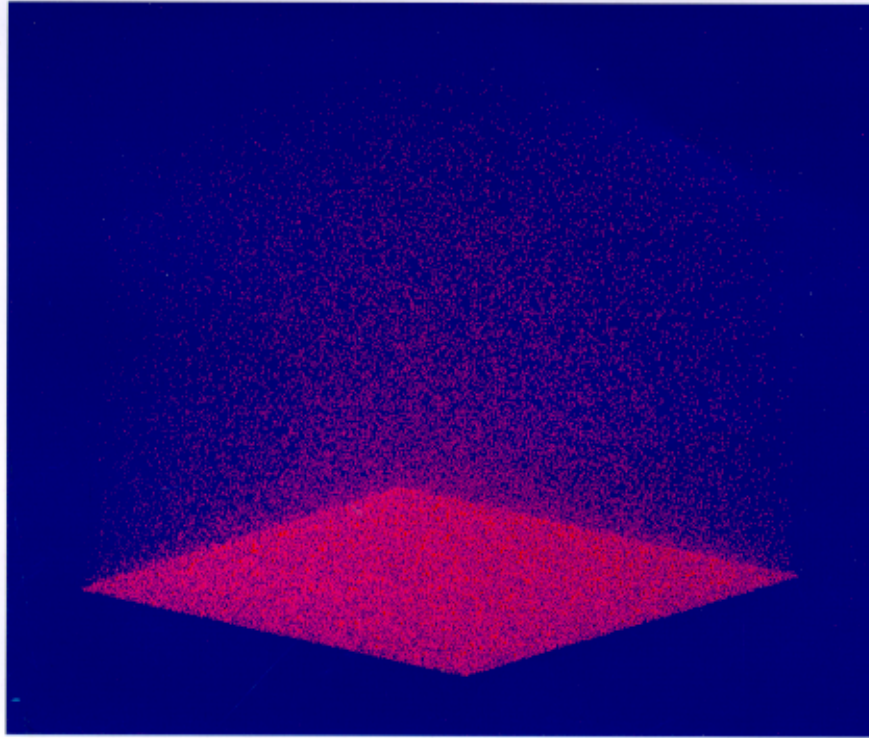


Fig. 4. The format of this orbit of a skew translation is the same as Fig. 1, the cat map. From a casual observation it is impossible to distinguish this orbit from the chaotic map in Fig. 1. However, the Lyapunov exponent is 0. In contrast to Fig. 2, a map with a positive Lyapunov exponent, this nonchaotic map more closely resembles chaos than the truly chaotic map of Fig. 2.

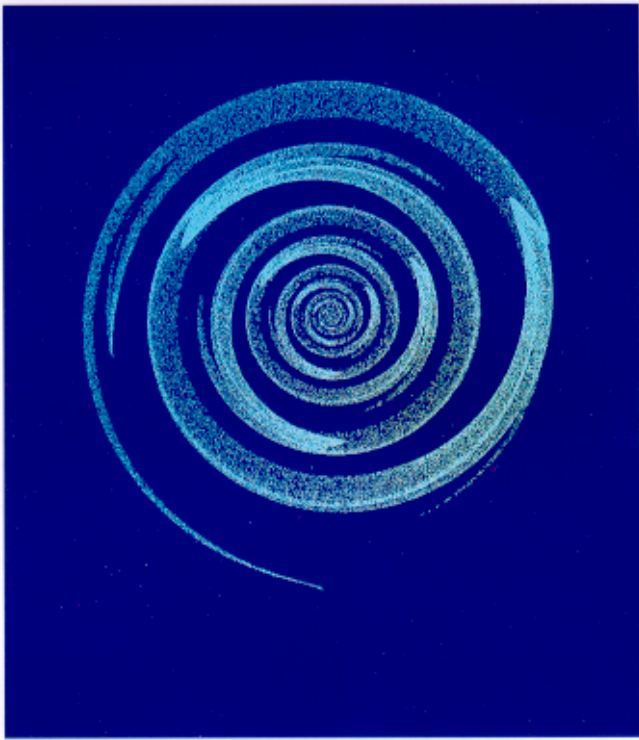


Fig. 5. In this figure we have transformed the orbit of Fig. 4 by a pair of twists. The result is a nonchaotic orbit that could be mistaken for a strange attractor.

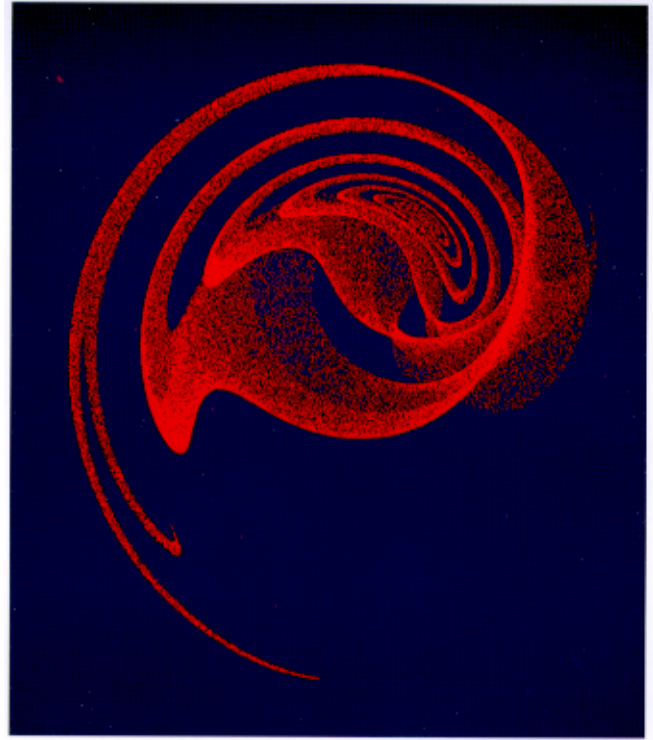
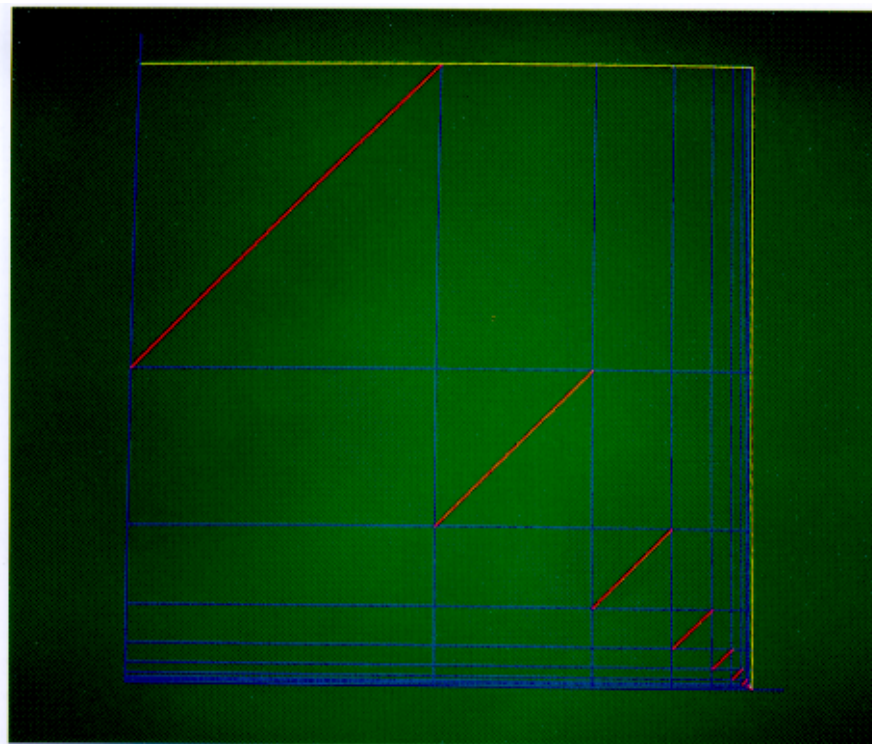
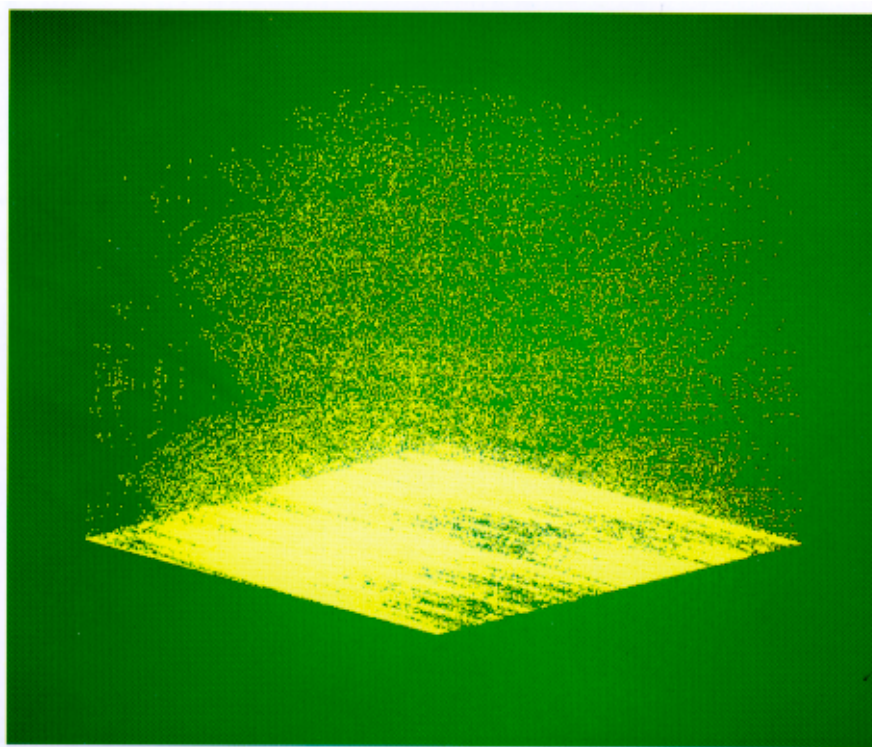


Fig. 6. In this figure we have transformed the orbit of Fig. 4 by another pair of twists, rendering a dramatic attractor which is nonchaotic.

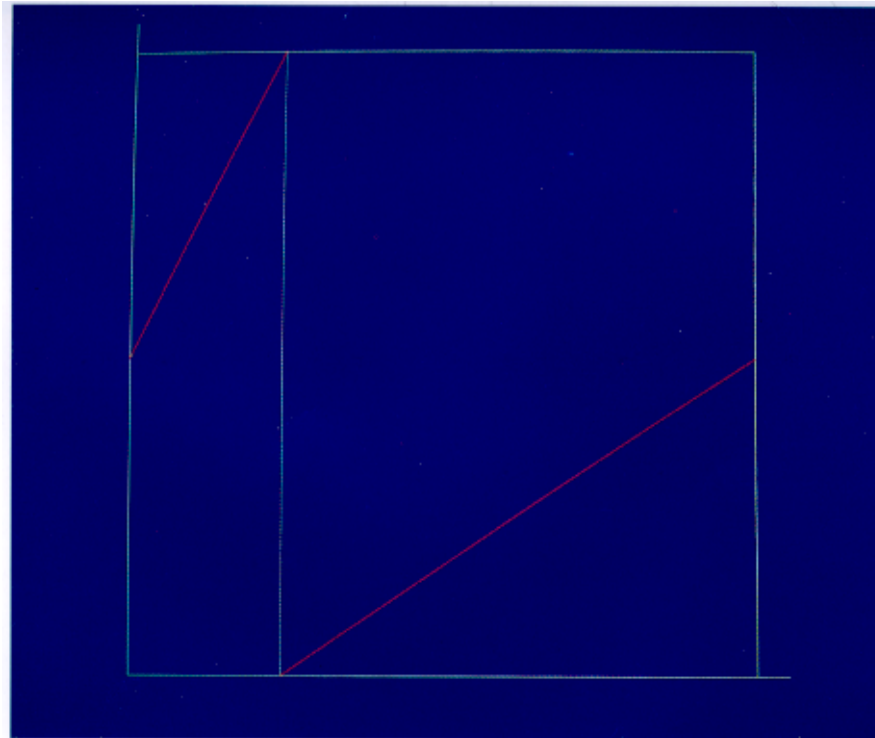


(a)

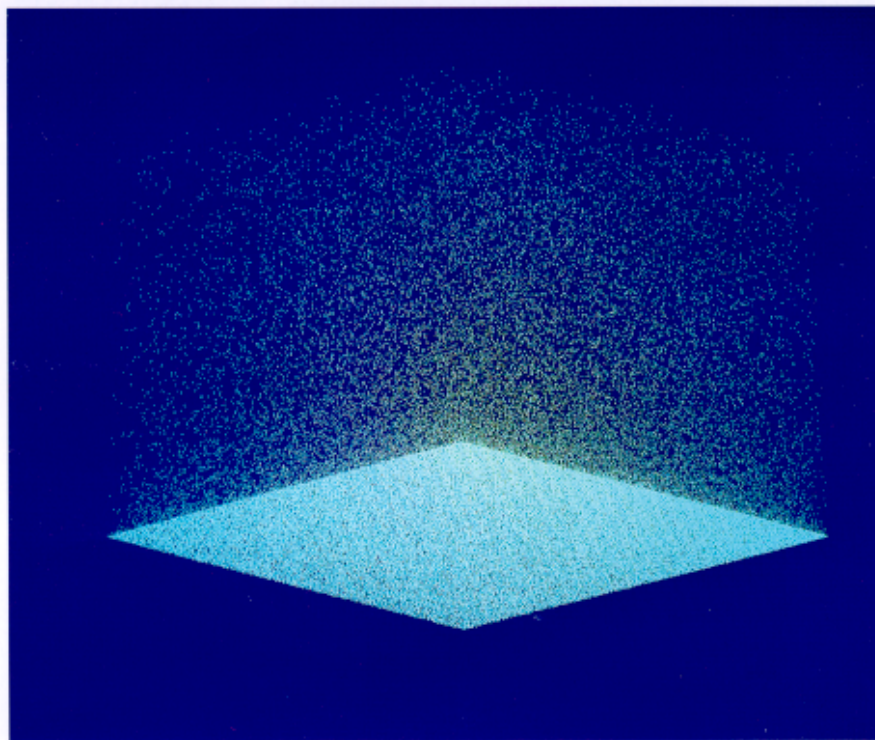


(b)

Fig. 7. (a) This figure is the graph of a simple ergodic map on the unit interval, an *interval exchange map* commonly encountered in ergodic theory. The x -axis partitions are at $(2^n - 1)/2^n$. The level of complexity here is minimal in that it is slightly more complicated than an irrational rotation. Except for the discontinuities, this map is made up of simple translations of intervals of the function $y = x$. (b) In this figure we have used the map of Fig. 7(a) to form a three-dimensional map in the format of Fig. 1. The orbit illustrated here shows just how complex this map can appear even though it is not chaotic.



(a)



(b)

Fig. 8. In Fig. 8(a) we construct a map, $g(x)$, with LZ and E. As a result, the computation of the Lyapunov exponent is reduced to the fundamental theorem of calculus and we see that the total percentage of expansion must equal the total percentage of contraction so that the net is 0. Figure 8(b) reveals that this map produces a distribution of orbit points that is quite uniform. The map for Fig. 8(b) is the same as Eq. (44) where f is replaced by g .

two twists:

$$T_1 \begin{pmatrix} w \\ z \end{pmatrix} = \begin{pmatrix} wz \\ z \end{pmatrix} \quad (39)$$

$$T_2 \begin{pmatrix} w \\ z \end{pmatrix} = \begin{pmatrix} w \\ zw \end{pmatrix} \quad (40)$$

and so

$$B \begin{pmatrix} w \\ z \end{pmatrix} = \begin{pmatrix} w^2z \\ zw \end{pmatrix} = T_2 \circ T_1. \quad (41)$$

The algebraic form of these equations reveals their relationships and clearly the skew translation falls between the twist (all orbits are almost periodic) and the Bernoulli map. If the complex number a has positive algorithmic complexity, the orbits of the skew translation are, relative to the twist, unpredictable and have sensitive dependence on initial conditions (SD). In fact, the real-valued coordinates of this skew translation have factors like $\sin(n^2)$, $\cos(n^2)$ which are uncorrelated. To see this we obtain the n th iterate of this map by a direct computation:

$$T^n \begin{pmatrix} x \\ y \end{pmatrix} = \begin{pmatrix} x + ny + n(n+1)a/2 \\ y + na \end{pmatrix} \text{mod}(1) \quad (42)$$

By considering k -dimensional skew translations we may obtain terms which behave like $\sin(n^k)$, while retaining E, ZA, SD, and LZ. Following this idea to its natural conclusion we can construct a map with LZ which has terms that behave like $\sin(p(n))$ where $p(n) \approx \exp(n)$.

Figures 4–6 illustrate some orbits of a skew translation. Figure 4 is the analog of Fig. 1 in Sec. 2 and is presented in the same way. The exact equation is

$$T \begin{pmatrix} w \\ z \\ u \end{pmatrix} = \begin{pmatrix} w + z \\ a + z \\ bu \end{pmatrix} \text{mod}(1) \quad (43)$$

where $0 < |a|, |w|, |z|, |b| < 1$. Note that using addition mod 1 is just a convenient way of coding this equation. We could use a five-dimensional equation in accordance with our developed techniques and obtain the same figure. The significance of this LZ, ZE map is that the spatial orbit structure in appearance is clearly more complex than that of Fig. 2 which was produced by a LP map.

Figure 5 is produced by using Eq. (43) with a coordinate transformation defined by a twisting

map. This demonstrates that an attractor's geometry can be separated from its level of complexity. Figure 6 demonstrates that other coordinate transformations can give the attractor any geometry we like. The specific coordinate transformation is not important. What is relevant is that the attractor can appear “strange” in one coordinate system while “familiar” in another.

Figure 7(a) illustrates a one-dimensional LZ map, $f(x)$. This example is due to Kakutani, see [Parry, 1981]. This map is far from chaos by any definition in that the orbits are slightly more complex than almost periodic orbits. But by making it a component of a three-dimensional map we reveal that it can produce an attractor which appears to have a high level of complexity, Fig. 7(b). The exact equation for Fig. 7(b) is as follows:

$$T \begin{pmatrix} w \\ z \\ u \end{pmatrix} = \begin{pmatrix} f(w) \\ z + w \\ au \end{pmatrix} \text{mod}(1) \quad (44)$$

where $0 < |w|, |z|, |b| < 1$. The “holes” in the attractor in Fig. 7(b) are not repelling regions, but rather reflections of the orbit correlation of the function f . If we iterate long enough, the entire square will be covered with the points of the orbit.

Taking a different turn we may ask if we can construct an example which is globally LZ for which there are times it is locally not LZ. This amounts to seeking an example which, when the exponents are averaged over infinite time, the exponents are not positive, but for which over finite periods of the orbit they are positive. Clearly, if there are some runs of positive exponents there must be some runs of negative exponents to force the average to be zero.

It is possible to construct any number of such maps on the unit interval so long as we allow a countable number of discontinuities. The process requires that the interval be partitioned into subintervals and on each subinterval we define our function to be increasing and differentiable. Further, on the set of subintervals the functions must be chosen to be invertible. Figure 8 is an example.

In Fig. 8(a) we construct a map, $g(x)$, with LZ and E. As a result, the computation of the Lyapunov exponent is reduced to the fundamental theorem of calculus and we see that the total percentage of expansion must equal the total percentage of contraction so that the net is 0. Figure 8(b) reveals that this map produces a distribution of orbit points that is quite uniform. The

map for Fig. 8(b) is the same as Eq. (44) where f is replaced by g .

Thus there are LZ maps which are WX, SD, and ZA, but are not B or even K . It is not known whether the map of Eq. (36) is SX for the right choice of a . These maps can be made Poincaré maps for ODEs which can be implemented in useful electronic circuits by the techniques of Brown and Chua [1993].

4. Strange Attractors and Space-Time Chaos

4.1. The phenomena of strange nonchaotic attractors

Numerous researchers have reported on strange nonchaotic attractors. An early paper is that of Grebogi *et al.* [1984]. The paper of Ding *et al.* [1989] is an important development of the 1984 paper. The authors sought to bring attention to the fact that an attractor may have complex geometry without arising from LP maps. The 1989 work sought to show how this fits into the scheme of nonlinear dynamics. We show here that the matter of

nonchaotic strange attractors can be traced to low-orbit correlation. But first we address the 1984 and 1989 examples.

The skew translation of Eq. (36) may be modified to be nonlinear as follows:

$$\begin{pmatrix} x \\ y \end{pmatrix} \rightarrow \begin{pmatrix} f(x, y) \\ y + a \end{pmatrix} \text{mod}(1) \quad (45)$$

where a is a constant. We remind the reader that the use of the mod(1) function is only a convenience and may be replaced by elementary functions by increasing the dimensions of our space. From this equation it is clear that the equations of Grebogi *et al.* [1984] are nonlinear skew translations as is also the case with the equations of Ding *et al.* [1989]:

$$\begin{pmatrix} x_{n+1} \\ \theta_{n+1} \end{pmatrix} = \begin{pmatrix} f(x_n, \theta_n) \\ (\theta_n + 2\pi\omega) \text{mod}(2\pi) \end{pmatrix}. \quad (46)$$

As with proving that maps are chaotic by proving the existence of horseshoes, for this line of analysis to be complete it would be necessary to show that the time-one maps of the ODE that are analyzing

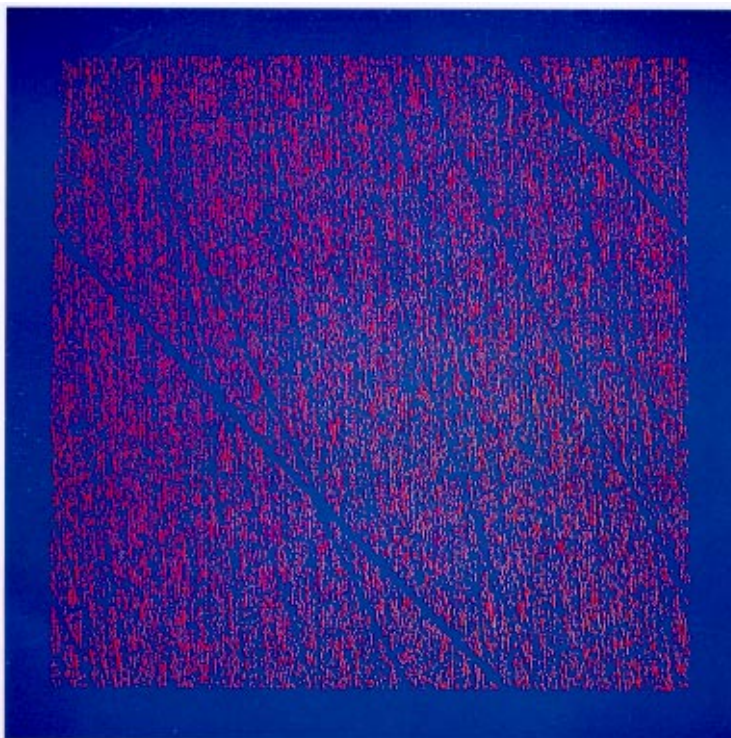


Fig. 9. Figure 9 demonstrates that the nonlinearities of the Grebogi, Ott, Pelikan and Yorke nonchaotic SA are not essential to obtain nonchaotic strange attractors. To obtain this attractor we have modified Eq. (36) to have an eigenvalue of 0.9999.

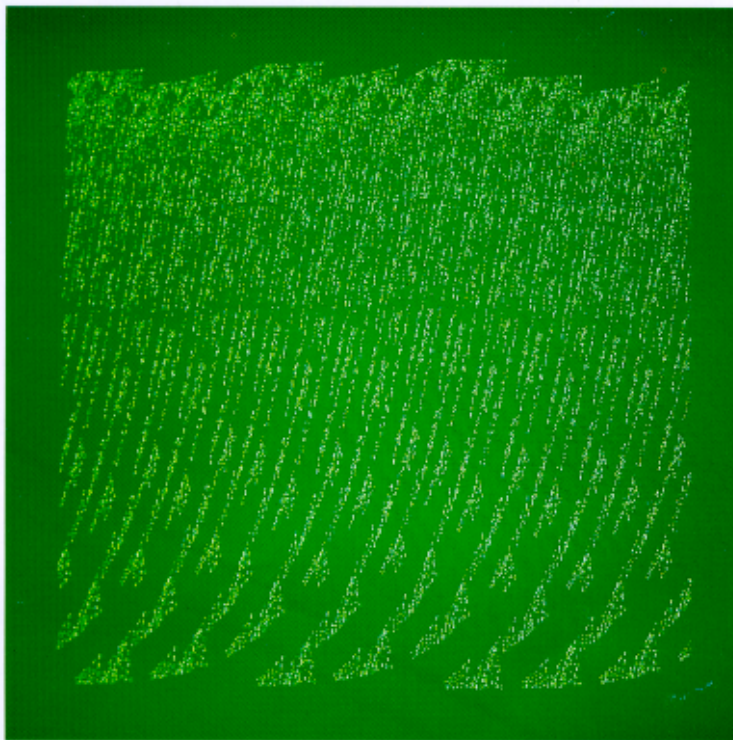


Fig. 10. Figure 10 is obtained by introducing a nonlinearity into the equation used to obtain Fig. 9. Introduction of the nonlinearity results in the formation of bending in the attractor.

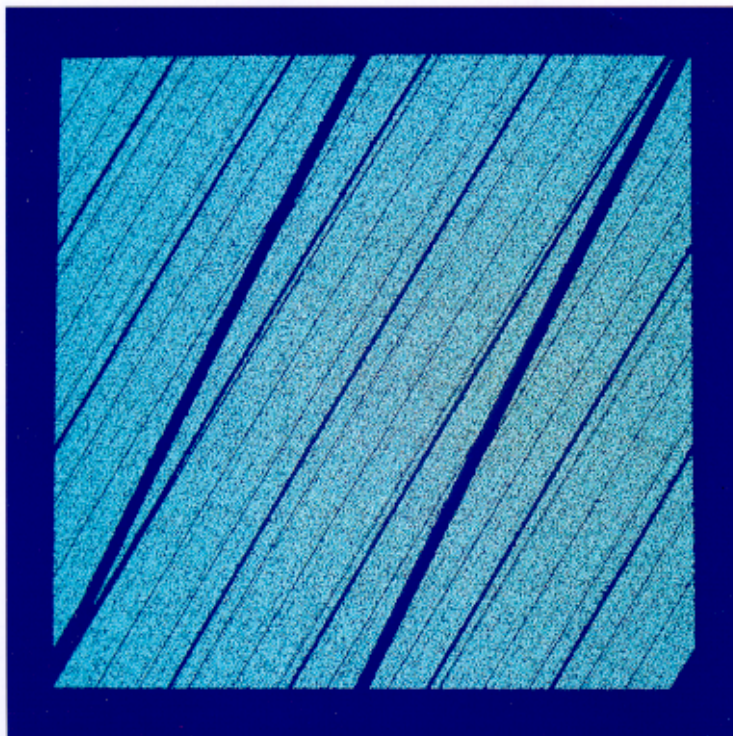


Fig. 11. In this figure we show that the process used to obtain a nonchaotic SA in Fig. 9 can also be used to produce a chaotic SA. Figures 9 and 11 demonstrate that the effect of damping is to reduce the level of complexity.

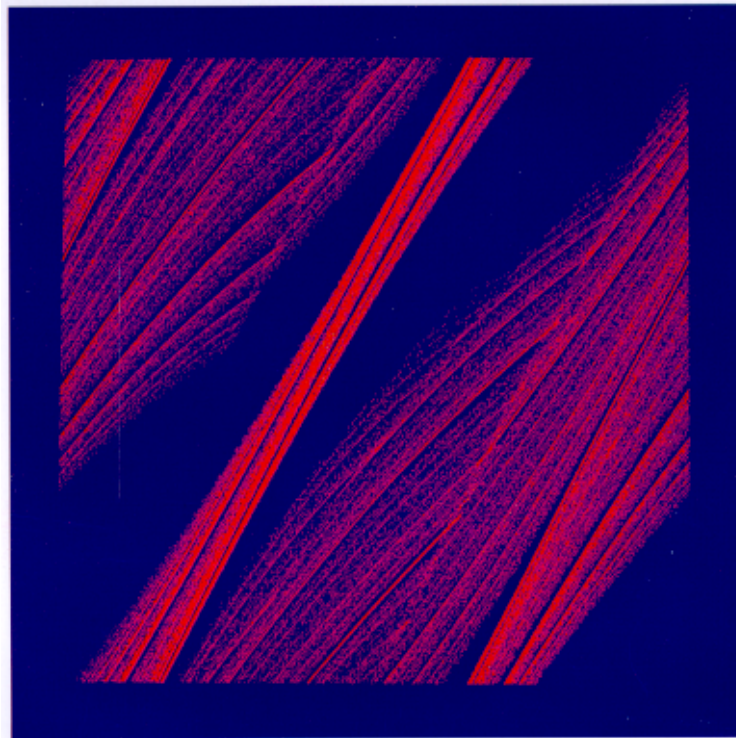


Fig. 12. This figure is made from Fig. 11 in the same way that Fig. 10 is made from Fig. 9, by introducing a nonlinearity. The result is the same: The nonlinearity introduces bending into the attractor.

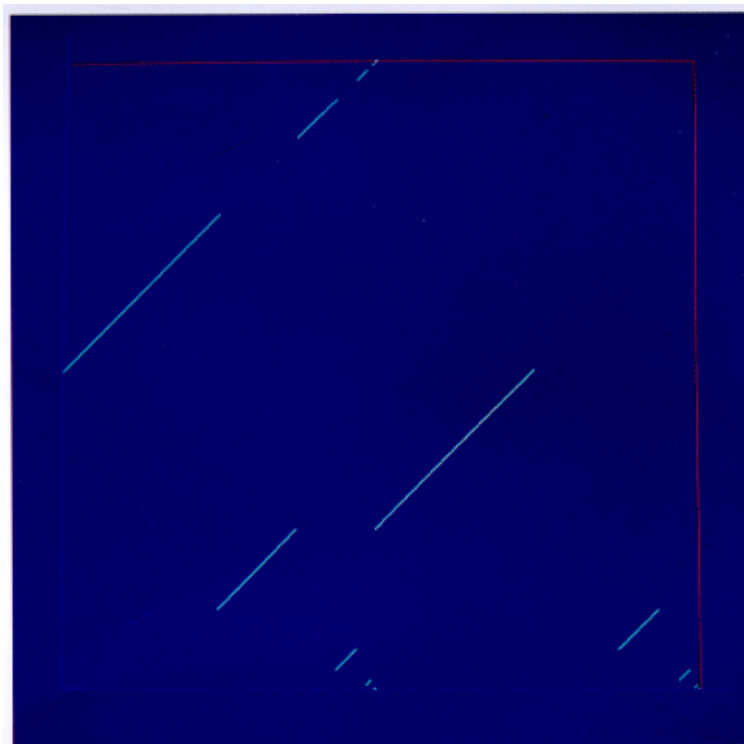


Fig. 13. This figure is a graph of a WX mapping, $x \rightarrow f(x)$, which is not SX constructed by Kakutani. It is LZ. All eigenvalues are 1, hence this map does no stretching.

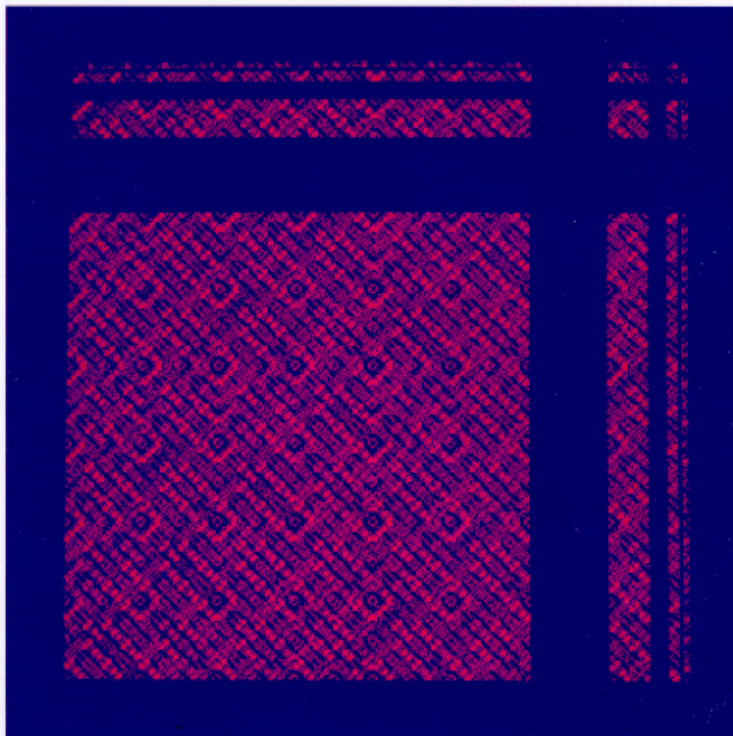


Fig. 14. In this figure we show an orbit of a map constructed from the map of Fig. 13. To get a two-dimensional image, we have formed the cross product of this mapping with itself, $(x, y) \rightarrow (f(x), f(y))$. The resulting mapping is also WX and LZ. The orbit shows a high degree of structure. A microscopic examination shows that the orbit has some level of complexity as well.

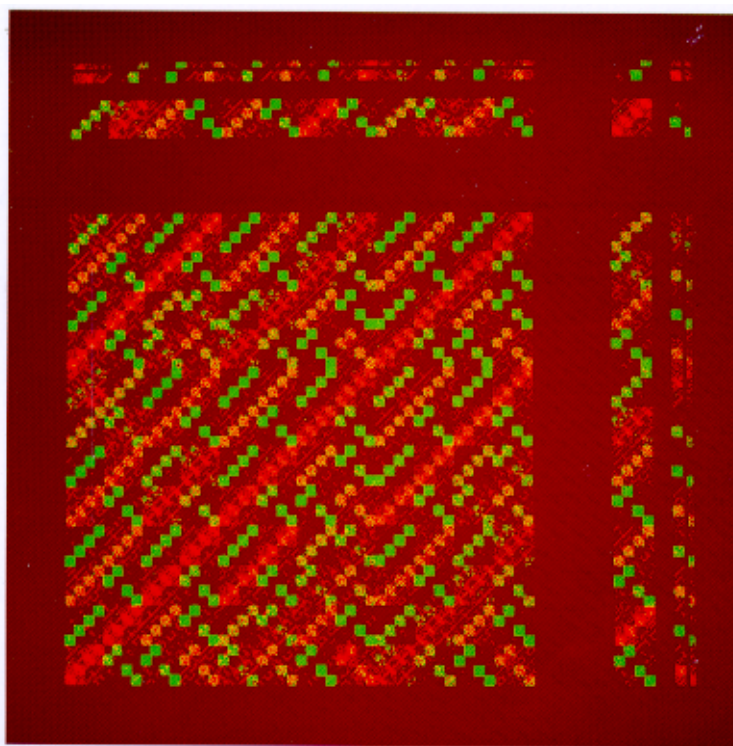


Fig. 15. In this figure we add a small measure of damping to the map in Fig. 14. The resulting map is $(x, y) \rightarrow (f(x), 0.999999 f(y))$. Several orbits are shown, distinguished by different colors. Since the orbits are not standard curves, they are nonchaotic strange attractors.

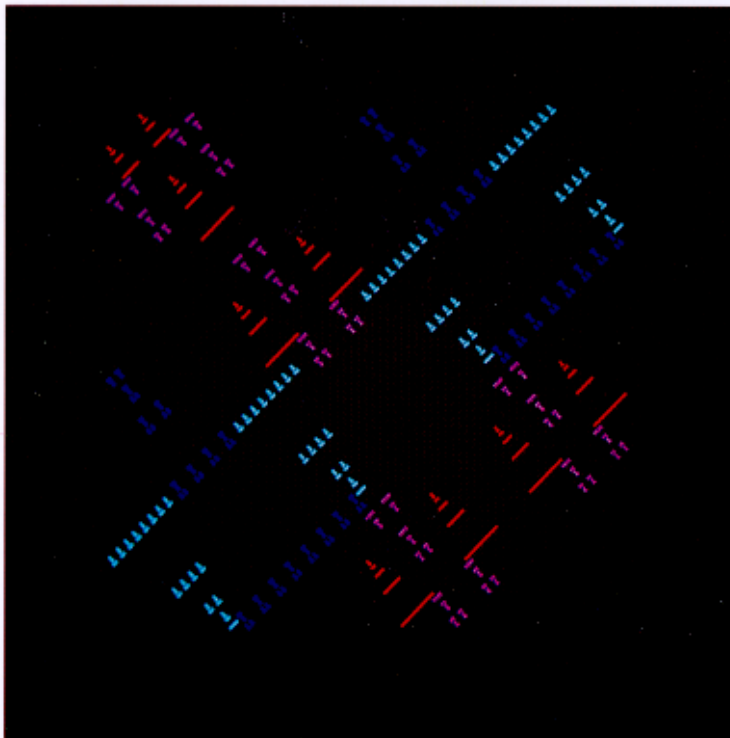


Fig. 16. This figure is constructed from the map in Fig. 7(a) by forming the direct product as we did in constructing Fig. 14 from Fig. 13. Four orbits are shown as indicated by the four colors. The presents of multiple distinct orbits shows that the map is not E.

are conjugate to a skew translation on some subset of its domain.

We now demonstrate that the nonlinearities of their maps are irrelevant to the existence of non-chaotic strange attractors. We modify Eq. (36) to have an eigenvalue less than 1:

$$\begin{pmatrix} x \\ y \end{pmatrix} \rightarrow \begin{pmatrix} \alpha x + y \\ y + a \end{pmatrix} \text{mod}(1) \quad (47)$$

and obtain the attractor in Fig. 9.

By making the map nonlinear we can routinely introduce bending into the attractor [Fig. 10].

The explanation of the formation of nonchaotic strange attractors is that if the orbits of a map are uncorrelated in time, the geometry of the orbit can become uncorrelated in space. Skew translations can have ZA, and hence their dampened orbits can be made to look peculiar, depending on how the damping factor is included in the equation of the map.

In general, in the presence of damping, the correlation of the orbits of a map can vary from 0 to 1, depending on the size of the damping factor, and this level of correlation may be reflected in the spatial geometry of the orbits. But note that printed

geometry, i.e. pictures, are a subjective element of human cognition, and what is peculiar is quite relative. It is possible to force the dampened uncorrelated orbits to take on familiar forms as well. Figure 4 demonstrates this. The attractor is a square. The effect on visual presentation of orbits is a function of *how* the damping is inserted in the equation. This distortion can happen for any map whose orbits lack some degree of correlation.

To further illustrate these ideas, if we modify the cat map to have damping, we may also get distorted attractor geometry as seen in Fig. 11.

The map for Fig. 11 is

$$\begin{pmatrix} x \\ y \end{pmatrix} \rightarrow \begin{pmatrix} 2x + y \\ x + (1 - 0.5\alpha)y \end{pmatrix} \text{mod}(1). \quad (48)$$

The parameter factor multiplying y is chosen to make the determinant of this map $1 - \alpha$. In Fig. 11, $\alpha = 0.02$.

By making the cat map nonlinear we cause the orbits to bend, as seen in Fig. 12.

The equation for Fig. 12 is

$$\begin{pmatrix} x \\ y \end{pmatrix} \rightarrow \begin{pmatrix} 2x + \sin(\beta y)^2 \\ x + (1 - 0.5\alpha)y \end{pmatrix} \text{mod}(1) \quad (49)$$

where $\beta = 1.8$. Figure 12 bears resemblance to the figures in [Brown & Chua, 1996b] where the fundamental map is presented. By construction, the fundamental map provides an orderly evolution from periodic to chaotic that encompasses skew translations and nonchaotic strange attractors. For the inverse of this idea, Fig. 1 is an example of a non-strange chaotic attractor in that the attractor is a square. It is possible to make a nonstrange chaotic attractor in the form a circle, straight line, or any simple geometric shape, except, possibly, a countable set of points.

Maps producing strange attractors have some level of complexity such as ZA, LP, or SD because the geometry is a reflection of orbit correlation. Thus the existence of strange attractors (SA) is a level of complexity we may add to our list of other measures. What we have seen is that the lower end of the level of complexity spectrum is periodic, and almost periodic dynamics. Next appears to be E, SD, WX, ZA, followed by LP. But this is not a totally ordered system, is it a partial order where SD is found in almost-periodic systems such as the twist on the two-dimensional torus. Of all the measures of complex dynamics, ZA and LP are the most general, but do not form a total ordering. Even by adding entropy we cannot obtain a single set of characteristics forming a total ordering. Either nature is being very capricious, or we just have not yet found the right measurements.

Relative to rotations, skew translations are quite complex, so we now ask the question *How low a level of complexity is needed to get SA?*. We present two examples. We begin with the WX map of Kakutani, see [Parry, 1981]. WX is mildly complex, but much less so than skew translations may be. Further, WX does not have to involve any stretching, contrary to what some authors have suggested. In fact the map of Kakutani is LZ [Fig. 13].

We present only the geometric form of this map due to its complicated definition found in [Parry, 1981]. Since this map is WX, its cross product is also WX and this is illustrated in Fig. 14. As can be seen, there is a large measure of global structure to an orbit, but on the detail level there is ample variation. If iterated long enough, the orbit will be dense, so the “empty” places in the figure do not indicate repelling regions.

By adding a small amount of damping, we get the attractor in Fig. 15, which may be termed strange.

Our last example of the phenomenon of non-chaotic SA demonstrates the considerable level of order that may be present and still obtain SA. We take the map of Fig. 7(a) to construct a strange attractor. This map, also constructed by Kakutani, is only E, and further, it has only discrete spectrum [Parry, 1981]. In simple language this means that among all E maps this type of E map is the simplest. For example, it is known that all E maps with discrete spectrum are group rotations. To obtain a two-dimensional illustration we form the cross product of this map with itself, and include a parameter, α , we can vary:

$$\begin{pmatrix} x \\ y \end{pmatrix} \rightarrow \begin{pmatrix} f(x) \\ \alpha f(y) \end{pmatrix}. \quad (50)$$

In Fig. 16, $\alpha = 1.0$, we show typical orbits of this map, which is not E, hence orbits are not dense. The different orbits are indicated by different colors. The orbits of f have a level of correlation ranging

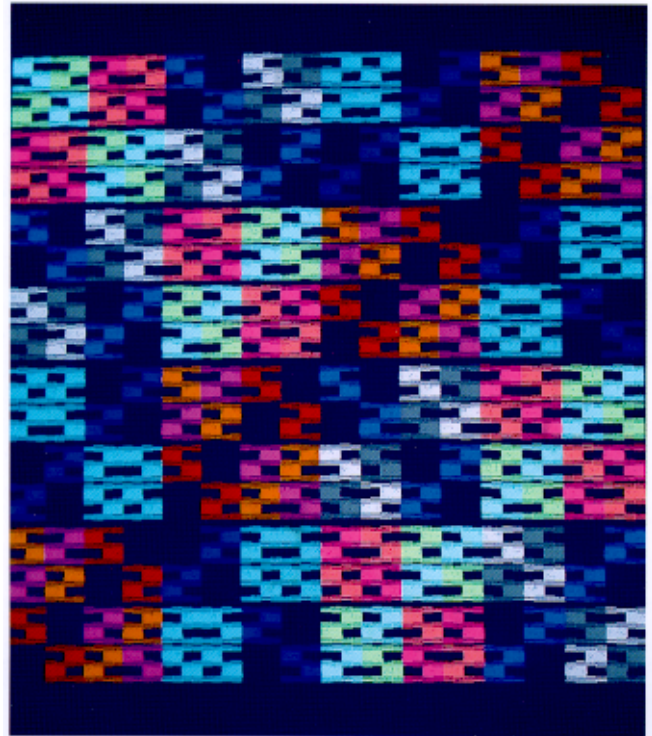


Fig. 17. This figure is obtained from Fig. 16 exactly as Fig. 15 was obtained from Fig. 14, by adding a small measure of damping to one coordinate, $\alpha = 0.999$. The result is the formation of nonchaotic strange attractors. Numerous orbits are shown as distinguished by the different colors. All orbits are strange in shape. This may be the weakest level of dynamics that can form nonchaotic strange attractors.

from about 0.55 to over 0.90, and the autocorrelation is nearly periodic.

In Fig. 17 we choose $\alpha = 0.999$, which is enough damping to form attractors. Figure 17 shows that the basins of attraction are in the shape of a block letter “S”. There are multiple basins, as indicated by the numerous colors, but some colors have been used twice. This is not important, however, since the point is that the various attractors are peculiar in shape, all have about the same shape, and there are many basins of attraction.

We conclude that the strangeness of the geometry of an attractor plotted on a computer screen is a result of the amount of damping, how the damping occurs in the definition of the map, and most important, the correlation of orbits. The exact value of the initial conditions may be a factor also. Clearly, the association of SA with chaos is a coincidence of the orbit correlation found in chaos. The level of complexity found in chaos and even in skew translations is far more than needed to obtain this interesting phenomenon.

4.2. *Initial conditions versus algorithms*

The examples of the preceding sections have demonstrated the need to determine when two points are correlated. We may define correlation of two points as follows: We first discard their integer part and consider only the fractional part of the number. We now consider their fractional part as a sequence of integers between 0 and 9. As sequences, we may apply the usual formula for correlation of two sequences to obtain the desired definition.

Using this definition, we have the following observation whose proof poses no mathematical difficulties.

Let x_0 be any point in space, and let $U(x_0)$ be any neighborhood of x_0 , however small. Then within $U(x_0)$ there are many points that are uncorrelated to x_0 .

This means in simple terms that near any point are countless points that are uncorrelated with it and that the location of the uncorrelated points is in essence a random walk from x_0 .

The significance of this fact is that any dynamical system that acts on two uncorrelated points in such a way as to move the insignificant, lower-level, digits up into a higher position of significance will be reflected in a complex relationship between the orbits of these two points. Hyperbolic systems are

capable of doing this. The shift is defined to do precisely this and nothing more. Different algorithms have varying abilities to elevate the role of lower-level digits into significance, and this is reflected in our notions of E, WX, SX, etc. The significance of this reaches a maximum when applied to points having positive algorithmic complexity. These are points which cannot be described by a finite algorithm and hence, cannot be reached by finite iteration of a finite algorithm. Such points cannot be spatially correlated to points having zero algorithmic complexity. For example, any dynamical system which moves lower-level digits into significance has a level of complexity of its orbit solely as a result of the algorithmic complexity of its initial condition. We may think of this as the extreme of spatial complexity. The lack of correlation between two points each with zero algorithmic complexity is philosophically less extreme.

Any dissipative dynamical system that treats uncorrelated points differently and correlated points similarly can have many basins of attraction as well as very complex-looking attractors.

We have traditionally viewed distance, i.e. metrics, as our primary measure of significance. However, correlation between points appears to hold an equally significant role in science and is more responsible for the levels of complexity we see in the universe than anything except those dynamical systems that elevate the lower-levels of complexity of points into positions of significance.

As a result, at least two numbers are necessary when comparing two quantities: their distance apart and their correlation. Their distance is a measure of the present; their correlation is a measure of their potential future relationships. Of these two measurements, clearly correlation is the most illusive and accounts for much of the uncertainty of the future. When two quantities are uncorrelated, their future depends solely on the type of dynamics they undergo. In weather systems, dynamics can fluctuate drastically from almost periodic upward, and thus uncorrelated quantities can fluctuate from having an almost-periodic relationship to a near-random relationship.

We have talked of uncorrelated quantities without being specific about the level of *uncorrelation*. Consequently, we ask: *How is the level of correlation between quantities reflected in their future under given dynamical systems?*

A simple question that we can answer is whether a simple rational or integer-initial

condition can converge to something complex, but not having positive algorithmic complexity, under the action of a dynamical system. The answer is yes. Any algorithm for the computation of the digits of π is an example. As noted in Part I of this tutorial, published last year, the Chudnovsky brothers have shown that the digits of π are as complex as the outputs of typical random-number generators. Next we ask if we may construct an algorithm having multiple basins of attraction which converge to two different “complicated” irrational numbers. The answer is yes, and the number of attractors may be made as large as you like. A typical example is

$$x \rightarrow h_1(x)f(x) + h_2(x)g(x) \quad (51)$$

where $f \rightarrow \sqrt{2}$, $g \rightarrow \sqrt{63}$ and $h_1(x)$ is 1 near $\sqrt{2}$ and 0 near $\sqrt{63}$, and $h_2(x)$ has the opposite specifications. If we start near either square root with a simple rational initial condition we converge to that square root, an irrational number. Hence it is a fact that we can use a finite algorithm to start at a simple initial condition and then, using this algorithm, be attracted to a complicated irrational number that tells us that dynamical systems can create some level of complexity, but not positive algorithmic complexity. We conclude that time can create a level of complexity and that space has an initial relative level of complexity. The spatial level of complexity is made more elusive by the mathematical fact that points exist with positive algorithmic complexity. The center of mass of a particle which is not initially located at a point of positive algorithmic complexity in a fixed-coordinate system can reach such a point — if the laws of nature have an expression as a finite algorithm — in only one of two ways: The algorithm involves a constant of positive algorithmic complexity, which contradicts its finite characterization; or it reaches the point at a moment in time of positive algorithmic complexity. However, particles having a center of mass with rational coordinates can converge to points having very complex coordinates in time under the action of a dynamical system that is expressible as a finite algorithm, regardless of the role of the time-coordinate.

We emphasize that the conclusions drawn are based on the relative spatial positions of points in a fixed-coordinate system. If the laws of nature are truly expressible as finite algorithms, then infinitely small particles located at some points can never reach other points within the same coordinate

system in finite time. We repeat that this is significant only on a microscopic scale in which particles are vanishingly small. Hence, the *theory of chaos* implies a fine, complex structure of the fabric of the universe, if only in the abstract.

Our theory of chaos thus implies the existence of both a spatial and a temporal level of complexity. The spatial level of complexity is revealed by the degree of correlation between points and the absolute relative level of complexity of points within a fixed coordinate system. Temporal level of complexity is revealed by the action of finitely-describable dynamical systems on points located at perfectly simple coordinates such as rational or integer coordinates. The level of complexity of things thus emanates from these two sources through the myriad of dynamical systems that have varying abilities to move lower-level complexity of physical quantities into positions of significance for measurement and prediction purposes.

5. Sources of Nonlinearity

In [Brown & Chua, 1997] we described the complexity spectrum and noted that understanding this spectrum is prerequisite to understanding chaos. In order to fully understand the sources of levels of complexity in the complexity spectrum it is necessary to understand the sources of nonlinearity, a key feature in the production of a given level of complexity. Nonlinearity is not a necessary feature for the production of a level of complexity, as we saw in the previous section, but nonlinearities are among the most interesting sources of high levels of complexity.

The simplest venue within which to investigate the sources of nonlinearities is the two-dimensional autonomous ODEs. The only simpler venue could be one-dimensional ODEs, or maps, but we believe that this venue is harder to approach in a simple orderly manner than the two-dimensional systems because interesting one-dimensional maps are either not invertible or not continuous.

The Poincaré–Bendixon theory would appear to completely answer all questions about the class of two-dimensional autonomous ODEs; however, on closer examination we see that this theory provides no insight into the construction of equations with specific nonlinear features, nor does it even suggest an organization of this topic. It is the varying ways in which nonlinearities may occur in two-dimensional autonomous ODEs that will provide us

with the insight into the role that these systems play in the development of a level of complexity, not a classification of their periodic points as presented by Poincaré–Bendixon theory.

5.1. The twist equation

In Davis' *Introduction to Nonlinear Differential and Integral Equations* [1962] the dominant source of nonlinearities in ODEs is revealed as being the occurrence of nonlinear frequencies in the solutions of the ODEs. A simple example of this is the twist ODE

$$\begin{pmatrix} \dot{x} \\ \dot{y} \end{pmatrix} = r \begin{pmatrix} 0 & -1 \\ 1 & 0 \end{pmatrix} \begin{pmatrix} x \\ y \end{pmatrix} \quad (52)$$

where $r = \sqrt{x^2 + y^2}$. The time-one (or Poincaré) map is the simple twist map which was used to derive the twist-and-flip map, the first closed-form Poincaré map of an ODE having chaotic solutions. This equation was derived by asking the question: What is the simplest way in which a linear equation can be made nonlinear? Since, in the linear oscillator the initial conditions determine the amplitude of the system, a simple step would be to consider the family of curves given by

$$\begin{pmatrix} x(t) \\ y(t) \end{pmatrix} = \begin{pmatrix} r \cos(rt + \theta) \\ r \sin(rt + \theta) \end{pmatrix} \quad (53)$$

where r is given above and is a function of the initial conditions. Since r affects both amplitude and frequency, the ODE that this system solves must be nonlinear. The effect of multiplying t by a function of the initial conditions is to cause neighboring orbits to separate, at different speeds. The orbits of the twist ODE in the phase plane are identical to those of the linear equation it was derived from. This procedure was shown to be very general in [Brown & Chua, 1993]: Given any linear autonomous ODE in any number of dimensions there is an infinite family of nonlinear autonomous ODE having the same set of orbits, fixed points, and types of fixed points.³ The solutions differ only in that, in the nonlinear case, t is multiplied by a function of the initial conditions that are constant along orbits.

³This fact alone shows that the classification of periodic points and limit cycles is inadequate to describe the nonlinear dynamics of two-dimensional autonomous systems.

⁴As is known, when this later second order ODE is driven by a periodic force, it produces chaos. In fact $\ddot{x} + x^3 = a \cos(t)$ is Duffing's equation without the damping term.

5.2. Example two: Nonlinear amplitude equation

We now ask if it is possible to generate a nonlinear system in which t is not multiplied by a function of the initial conditions but whose amplitude is a function of the initial conditions. The answer is yes, and the ODE is derived from the curves given by

$$\begin{pmatrix} x(t) \\ y(t) \end{pmatrix} = \begin{pmatrix} r \cos(t + \theta) \\ r^2 \sin(t + \theta) \end{pmatrix} \quad (54)$$

where r is a function of the initial conditions given by $r^2 = 0.5(x^2 + \sqrt{x^4 + 4y^2})$. By direct computations the following system of autonomous ODEs can be derived:

$$\begin{pmatrix} \dot{x} \\ \dot{y} \end{pmatrix} = \begin{pmatrix} 0 & -1/r \\ r & 0 \end{pmatrix} \begin{pmatrix} x \\ y \end{pmatrix} \quad (55)$$

where $r^2 = 0.5(x^2 + \sqrt{x^4 + 4y^2})$ is a constant along integral curves. This system has a feature in common with the ODE $\ddot{x} + x^3 = 0$ in that the shape of the integral curves varies with the initial conditions [Fig. 18]. The twist equations also have a feature in common with this second order ODE: The frequency varies with the initial conditions. However, in the twist equations, the solutions are all circles, thus the amplitude is essentially what we expect from a linear system. In the amplitude system, the frequencies are not a function of the initial conditions. Hence, the twist equations and the amplitude equations have completely separated two of the three features of nonlinear systems illustrated by $\ddot{x} + x^3 = 0$. The third feature, variable velocity along points of a single orbit, will be discussed in the next example.⁴

A natural question is whether the amplitude equation with periodic forcing produces chaos as well. The answer is yes.

By a direct computation a time-one or Poincaré map can be derived for the amplitude equation:

$$\mathbf{A} \begin{pmatrix} x \\ y \end{pmatrix} = \begin{pmatrix} \cos(\theta) & -\sin(\theta)/r \\ \sin(\theta)r & \cos(\theta) \end{pmatrix} \begin{pmatrix} x \\ y \end{pmatrix} \quad (56)$$

where θ is a fixed time interval. The orbits of this map are ellipses [Fig. 18]. For small initial

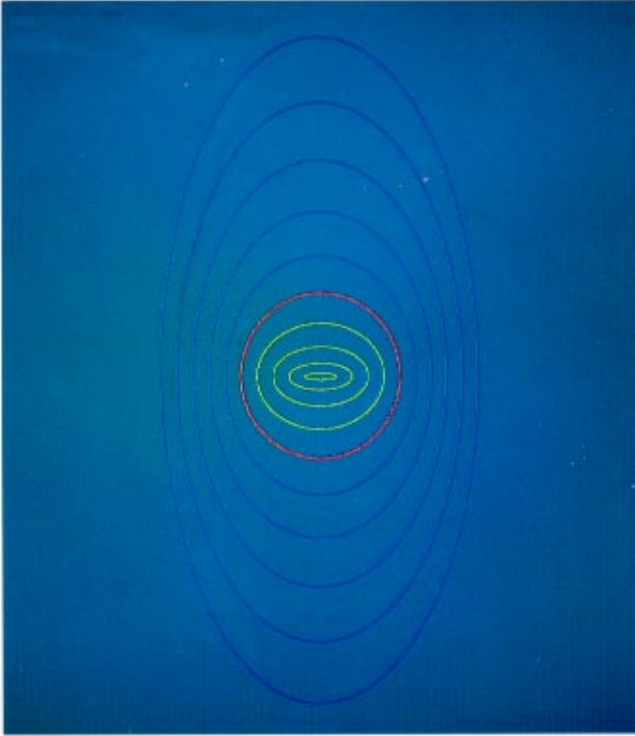


Fig. 18. In this figure we show the orbits of a nonlinear equation. Each orbit, considered by itself, is linear, varying from horizontal ellipses (yellow), to a circle (red), to vertical ellipses (dark blue). The relationship between the orbits is the source of the nonlinearity.

conditions the semi-major axis is horizontal (yellow orbits); for large initial conditions it is vertical (dark-blue orbits). Therefore one orbit is circular and, as seen in Fig. 18, red.

To obtain chaos using this nonlinear effect we must add forcing to the ODE, and this is done exactly as we did for the twist-and-flip equations. Doing this we can obtain a Poincaré map and have the analog of the twist-and-flip map which we will call FA. As with the twist-and-flip map we must offset the center of the integral curves by an amount a . After this is done our resulting map is

$$\mathbf{FA} \begin{pmatrix} x \\ y \end{pmatrix} = - \left[\begin{pmatrix} \cos(\theta) & -\sin(\theta)/r \\ \sin(\theta)r & \cos(\theta) \end{pmatrix} \begin{pmatrix} x-a \\ y \end{pmatrix} + \begin{pmatrix} a \\ 0 \end{pmatrix} \right] \quad (57)$$

and the orbits are seen in Fig. 19.

This map has no hyperbolic fixed points but does have high-order hyperbolic periodic points. For $\theta = 2.0$, $a = 0.5$ a period-six hyperbolic point is found at approximately $(1.0433, 1.1997)$. By direct inspection this point is found to have a horseshoe. This example illustrates the contribution of the geometry of the orbits to producing chaos.

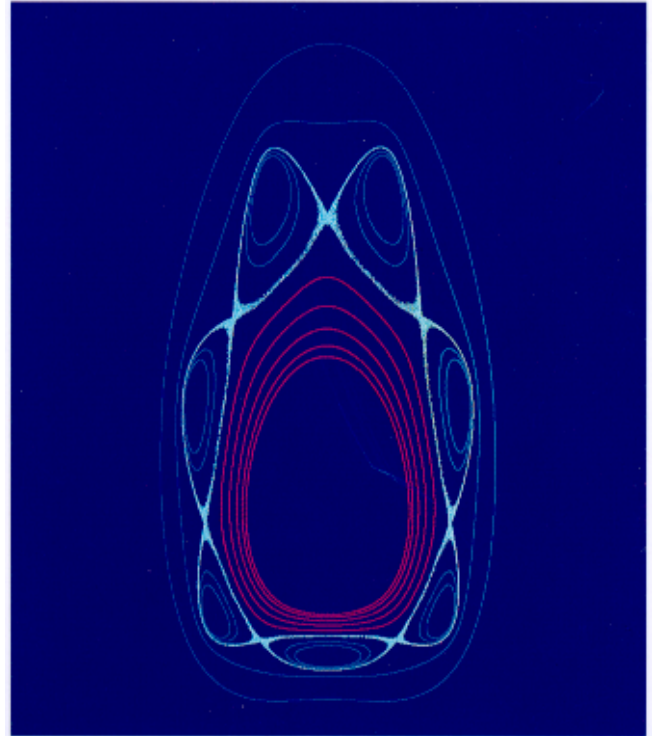


Fig. 19. In this figure, we demonstrate that by combining the map of Fig. 18 with a flip we obtain chaos, just as is done with the twist. As is shown in the figure, the full array of island chains (dark blue) and homoclinic tangles (light blue) are formed.

5.3. *Example three: The Jacobi equation*

All two-dimensional vector fields can be put into the form:

$$\begin{pmatrix} \dot{x} \\ \dot{y} \end{pmatrix} = \begin{pmatrix} \dot{r} \\ r \end{pmatrix} \mathbf{I} + \dot{\theta} \mathbf{B} \begin{pmatrix} x \\ y \end{pmatrix} \quad (58)$$

where \mathbf{I} is the identity matrix and \mathbf{B} is the matrix

$$\begin{pmatrix} 0 & -1 \\ 1 & 0 \end{pmatrix}. \quad (59)$$

When $\dot{r} = 0$ we get the equation:

$$\begin{pmatrix} \dot{x} \\ \dot{y} \end{pmatrix} = (\dot{\theta} \mathbf{B}) \begin{pmatrix} x \\ y \end{pmatrix} \quad (60)$$

the orbits must be circles, the same as the simple harmonic oscillator and the twist equation. For $\dot{\theta} = 1$ we obtain the simple harmonic oscillator. For $\dot{\theta} = r$ we obtain the twist. However, if

$$\frac{\partial \dot{\theta}}{\partial r} = 0 \quad (61)$$

we are still in a position to obtain closed-form solutions. If $\dot{\theta} = \sqrt{1 - k^2 \sin^2(\theta)}$ we obtain the closed-form solution

$$\begin{pmatrix} x(t) \\ y(t) \end{pmatrix} = \begin{pmatrix} r \operatorname{cn}(t + C) \\ r \operatorname{sn}(t + C) \end{pmatrix} \quad (62)$$

where sn , cn are the Jacobi elliptic functions. We call this the Jacobi Equation. These functions are the inverses of elliptic integrals and are derived in the classical problem of rectifying the ellipse.

Since $\dot{\theta}$ is not a function of r , the angular velocity does not change from orbit to orbit as was the case with the twist system. In fact, this system preserves lines through the origin and through any complete revolution a line or a region is mapped onto itself. The source of the nonlinearity is that along an orbit, the arc length is expanded and contracted in a periodic manner. In this system, matter is neither created, as happens in systems having a source, nor destroyed, as happens with systems having a sink, but rather is alternately compressed and stretched.

This system can be used to obtain chaos by the standard two-phase gate method: If we translate the system to $(a, 0)$ and compose it with the flip we obtain a Poincaré map that produces chaos while having only periodic hyperbolic points and no hyperbolic fixed points. The origin of chaos in this system is solely from the nonlinear acceleration taking place around circles.

A limitation of the Jacobi Equation is that the Jacobi elliptic functions, $\operatorname{sn}(t)$, $\operatorname{cn}(t)$ are not elementary functions. However, the time-one map determined by these equations can be constructed from elementary functions. For anyone wanting to proceed by constructing an example which avoids the use of the Jacobi Equation, we offer the following digression:

We may construct an example having these exact same properties which is solvable in terms of elementary functions. In place of $\dot{\theta} = \sqrt{1 - k^2 \sin^2(\theta)}$ we simply choose $\dot{\theta} = 2 - \sin^2(\theta)$, which is integrable in terms of elementary functions. Specifically, we have

$$\sin(\theta) = \frac{\sqrt{2} \sin(\psi)}{\sqrt{1 + \sin^2(\psi)}} \quad (63)$$

and

$$\cos(\theta) = \frac{\cos(\psi)}{\sqrt{1 + \sin^2(\psi)}} \quad (64)$$

where $\psi = \sqrt{2}(t + C)$, C being the arbitrary constant of integration determined by the initial conditions. Since $\dot{r} = 0$, we can write the solution in rectangular coordinates from the above information and the initial conditions. Specifically,

$$\begin{pmatrix} \sin(\psi) \\ \cos(\psi) \end{pmatrix} = \begin{pmatrix} C_1 \cos(\sqrt{2}t) - C_2 \sin(\sqrt{2}t) \\ C_1 \sin(\sqrt{2}t) - C_2 \cos(\sqrt{2}t) \end{pmatrix} \quad (65)$$

with

$$C_1 = \frac{\sqrt{2}x_0}{\sqrt{2x_0^2 + y_0}}, \quad C_2 = \frac{y_0}{\sqrt{2x_0^2 + y_0}}. \quad (66)$$

The significance of these systems as a building-block of a level of complexity is twofold. First, the nonlinear acceleration around orbits of these two equations, when composed with simple linear factors, gives rise to chaos even though the nonlinearity is of the simplest conceivable form, far simpler than the twist map in that it has no shearing. Second, two observers traveling on nearby orbits lying on the same radial line will not experience relative motion. Further, observers riding on separate orbits will never separate by more than a fixed but small distance. It is nearly the opposite of sensitive dependence on initial conditions. Two observers riding on the same orbit will oscillate relative to each other while still remaining in circular motion. This stretching and compressing of arc length around the orbit means that the vector field has a nonzero divergence while having no sources or sinks. Matter is never created or destroyed as when there are attractors or repellers involved; it is only compressed and stretched. The result of this feature is that when it is composed with simple components such as the flip, chaos is created by a subtle process. In addition, a very unexpected result appears: Local attracting periodic points are mixed in with periodic, quasi-periodic and chaotic orbits [Fig. 20]. This is due to the nonzero divergence of this system. If the divergence were a result of sinks or sources, we would expect to obtain global attractors or repellers. But this is not what is found. The existence of local attracting fixed points also depends on the magnitude of the flip component used to compose these maps. Only certain flips combined with the right initial conditions can give rise to this unusual phenomena. Figure 20 illustrates beautifully the kinds of orbits possible with the Jacobi map as a factor. The presence of measure-preserving chaotic and elliptic

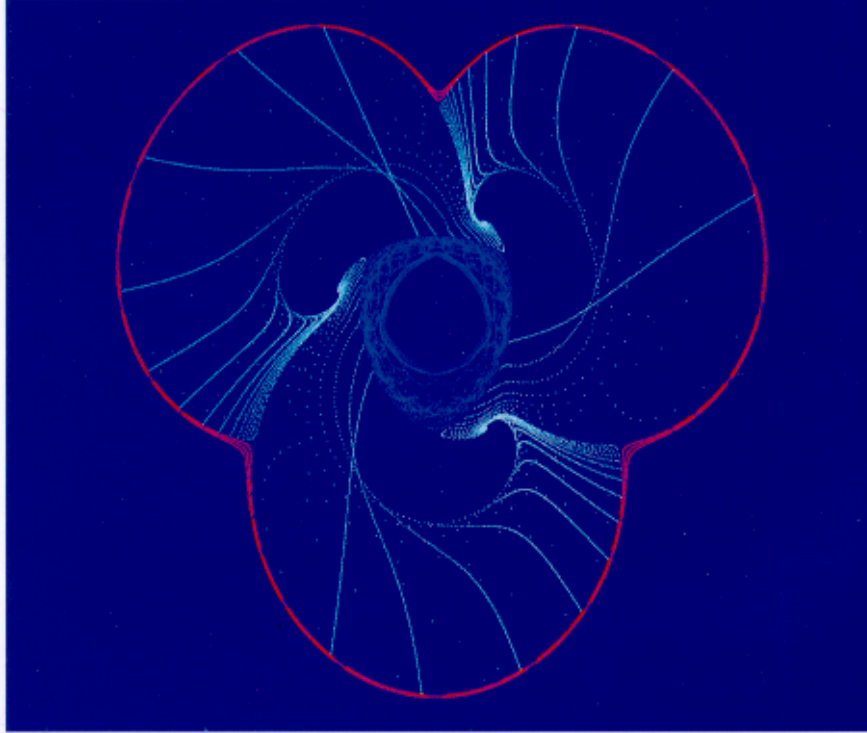


Fig. 20. Figure 20 is an example of a remarkable phenomena, the coexistence of local attracting periodic points (light blue orbits converge to period-three points) with nonattracting regions. A chaotic region having a homoclinic tangle is shown in red. This phenomena results from the nonzero divergence of the Jacobi equation.

orbits combined with period three attractors suggests the possibility of such systems existing in nature. The work of Freeman [1996] on the attractors of the brain combined with the nonattractor nature of common brain waves suggests that the brain is a system with these properties. This system may one day also explain how complex structures such as the spinal column can form from dynamical systems composed of simple components.

Three sources of autonomous, integrable nonlinearity in two dimensions are thus illustrated by these three equations: the twist equation, the amplitude equation and the Jacobi Equation. The twist equation is the most readily available source of chaos and it has zero divergence. The second of the two equations provides a source of asymmetry and subtlety not found in the twist equations and also has zero divergence. Two of these equations are induced by linear equations; all three have only linear orbits. In particular, the orbits are either ellipses or circles.

5.4. *Example four: Nonlinear orbits*

In the preceding three examples we imposed a

constraint that the individual orbits of the ODE be linear and observed that nonlinearity could arise from three different sources: nonlinear frequencies, nonlinear relationships between neighboring orbits, and nonlinear divergence. Another source of nonlinearity must be nonlinear orbits.

We now illustrate how to obtain a nonlinear system that: (1) can be solved in closed form; (2) is not induced by a linear system; (3) whose orbits are not linear; (4) which preserves lines through the origin; and (5) which has zero divergence. We use the form of a vector field mentioned above:

$$\begin{pmatrix} \dot{x} \\ \dot{y} \end{pmatrix} = \begin{pmatrix} \dot{r} \\ r \end{pmatrix} \mathbf{I} + \dot{\theta} \mathbf{B} \begin{pmatrix} x \\ y \end{pmatrix} \quad (67)$$

and make two assumptions. The first is that its underlying group is measure preserving or, what is the same thing, the vector field is divergence-free. The second is that the system preserves lines through the origin. Using these two assumptions we derive the following partial differential equation for \dot{r} :

$$\frac{1}{r} \langle X, \nabla \dot{r} \rangle + \frac{\dot{r}}{r} + \langle \mathbf{B}X, \nabla \dot{\theta} \rangle = 0. \quad (68)$$

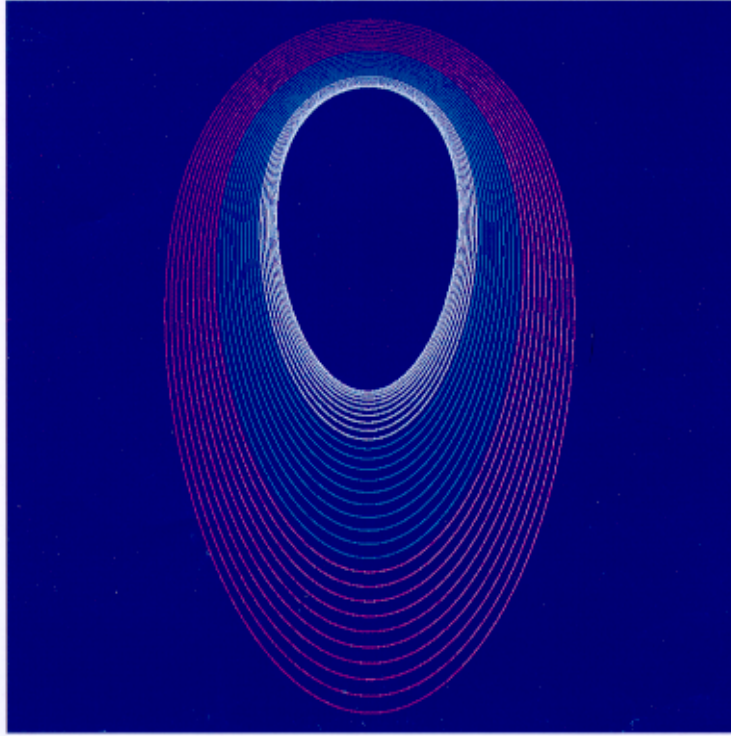


Fig. 21. Figure 21 illustrates the orbits of a nonlinear system that: (1) can be solved in closed form; (2) is not induced by a linear system; (3) whose orbits are not linear; (4) which preserves lines through the origin; and (5) which has zero divergence.

With the following notational convention we obtain the PDE in standard form. Let

$$\begin{pmatrix} \dot{r} \\ \dot{\theta} \end{pmatrix} = \begin{pmatrix} g(x, y) \\ f(\theta) \end{pmatrix}. \quad (69)$$

Now the PDE becomes

$$xp + yq = -(z + rf'(\theta)) \quad (70)$$

where $p = z_x$, $q = z_y$, $z = \dot{r} = g(x, y)$. The general solution is given by

$$z = h(x, y)F(x/y) \quad (71)$$

where h is dependent on $f'(\theta)$. If we assume that $cz = rf'(\theta)$ is the form of the solution, then we obtain the following consistency equation to check:

$$xp + yq = -(c + 1)z. \quad (72)$$

All of these assumptions would be fine if the solution of the resulting equation is consistent with these assumptions. By an application of standard methods for solving first-order partial differential equations we get

$$z = \frac{y}{-(c + 1)}F(x/y). \quad (73)$$

The consistency check we must make is to see whether

$$rf'(\theta) = \frac{y}{-(c + 1)}F(x/y) \quad (74)$$

is possible. Since $y = r \sin(\theta)$, $x = r \cos(\theta)$ we see that if we choose $f(\theta) = a + b \sin(\theta)$, everything is consistent. In particular, we have

$$r = r_0 \left(\frac{f(\theta_0)}{f(\theta)} \right)^{1/c} \quad (75)$$

and the first part of the solution is done. Now, if we choose $a > b$, the equation $\dot{\theta} = a + b \sin(\theta)$ is solvable in closed form for $\sin(\theta)$. Using a standard table of integrals we get

$$\frac{b + a \sin(\theta)}{a + b \sin(\theta)} = \sin(kt + C_0) \quad (76)$$

where $k = \sqrt{a^2 - b^2}$, and C_0 is a constant of integration to be determined from the initial conditions. From this relation we obtain $\sin(\theta)$, $\cos(\theta)$ and we are done.

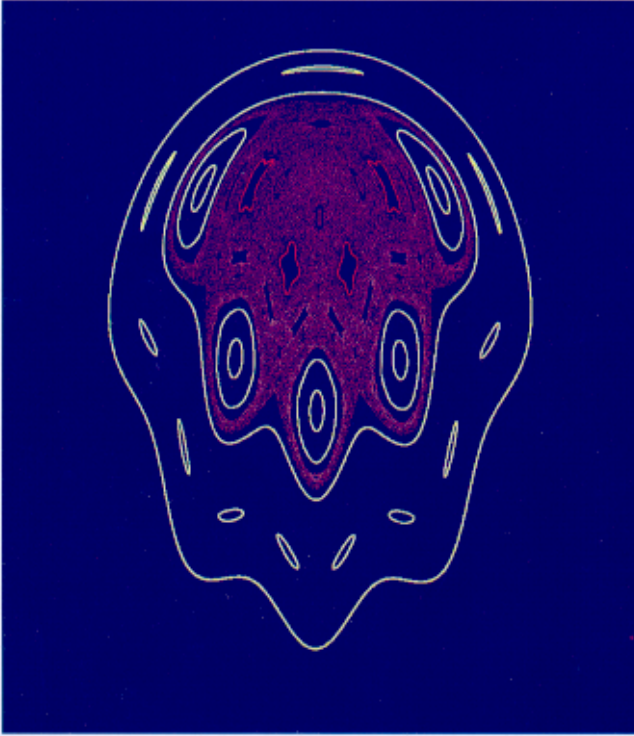


Fig. 22. In this figure we combine the map of Fig. 21 with a flip to obtain chaos. Familiar island-chains (red) and chaotic regions (blue) are formed.

The general solution in rectangular coordinates is given by:

$$\begin{pmatrix} x(t) \\ y(t) \end{pmatrix} = r_0 \left(\frac{f(\theta_0)}{f(\theta)} \right)^{1/c} \begin{pmatrix} \cos(\theta) \\ \sin(\theta) \end{pmatrix} \quad (77)$$

where we must have $c > 1$. Note that the root factor is not a constant since $f(\theta)$ is a function of time. The orbits cannot be linear, see Fig. 21, and, by construction, the system is divergence-free. Using the two-phase gate method, we may make this map a component of a Poincaré map which produces chaos [Fig. 22].

5.5. Example five: Nonzero divergence, with nonlinear orbits

It is possible to obtain nonzero divergence equations that are just as useful. One option is to solve the PDE $xp + yq = z$ and the choice

$$\dot{r} = -r f'(\theta) \quad (78)$$

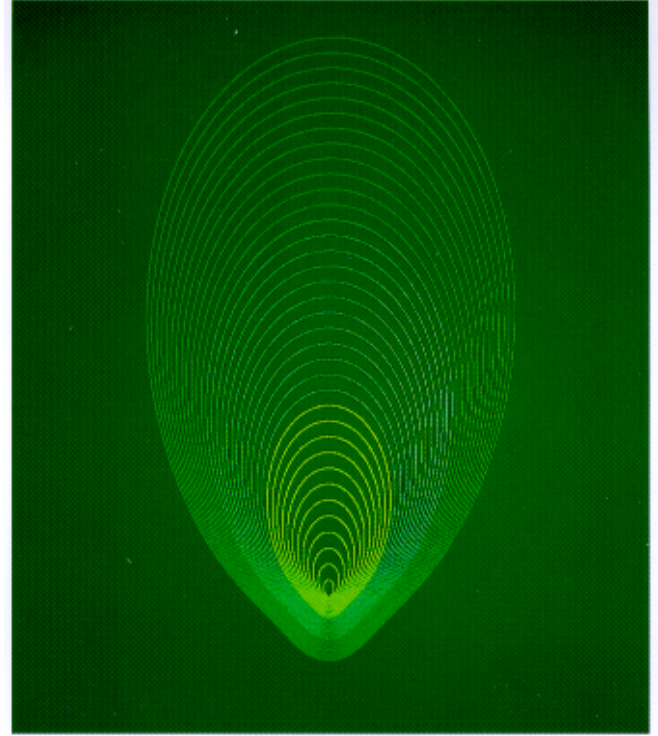


Fig. 23. Figure 23 illustrates the orbits of a nonlinear system that is the analog of Fig. 21, but which has nonzero divergence.

with $\dot{\theta} = f(\theta) \neq \text{constant}$ gives the closed-form solutions in rectangular coordinates:

$$\begin{pmatrix} x(t) \\ y(t) \end{pmatrix} = r_0 \frac{f(\theta_0)}{f(\theta)} \begin{pmatrix} \cos(\theta) \\ \sin(\theta) \end{pmatrix}. \quad (79)$$

Note that if $\dot{\theta} = -1$ and $\dot{r} \neq 0$ we also get nonzero divergence.

This process can be greatly generalized. If $\dot{\theta} = f(\theta)$ and $r = C_0 G(\theta)$ we get an autonomous ODE:

$$\dot{r} = C_0 G''(\theta) f(\theta) \quad (80)$$

where C_0 is eliminated from this equation by noting that $C_0 = r/G(\theta)$. So long as $\dot{\theta} = f(\theta)$ is solvable in closed form, we are done! For example, choose $f(\theta) = 2 - \sin^2(\theta)$. By use of a table of integrals we find that we can solve this equation for $\sin(\theta)$, which is all that is necessary to express the solution in rectangular coordinates. By choosing $G(\theta) = \sqrt{f(\theta)}(1 - 0.95 \sin(\sin(\theta)))$ we get the orbits of Fig. 23.

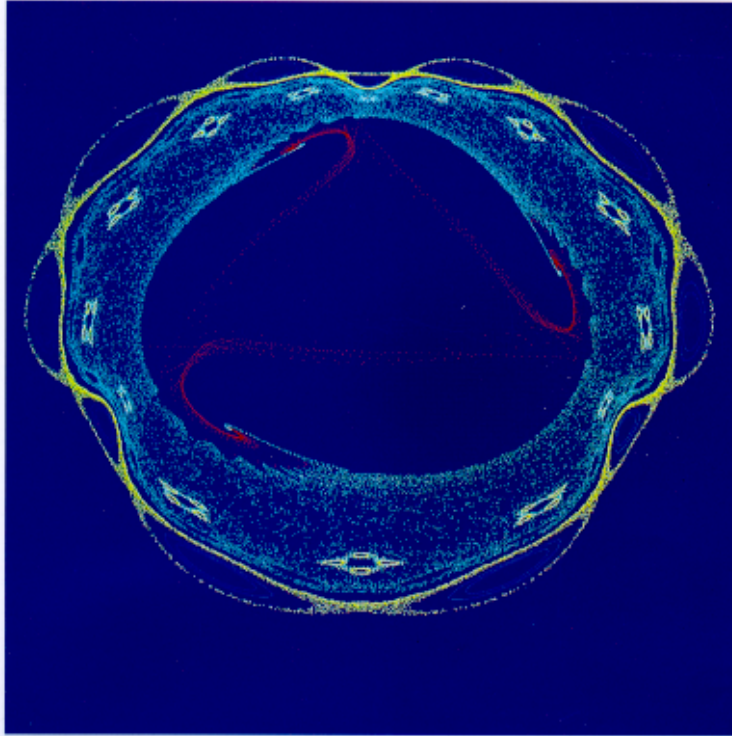


Fig. 24. In this figure, we compose the time-one map of Fig. 23 with a linear translation to get the Poincaré map for an electronic circuit using a two-phased gate. Just as in Fig. 20, local attracting periodic points form with nonattracting regions to produce a remarkable combination of dynamics: In dark blue are elliptic regions; in light blue and yellow are chaotic regions containing homoclinic tangles; in red are orbits that converge to a set of period-three points.

By composing this autonomous time-one map with a shift, we get the chaotic orbits of Fig. 24.

This system, like the Jacobi Equation, when composed with linear maps by the method of two-phase gates can generate local attracting fixed points alongside periodic, quasi-periodic, and chaotic orbits which are not attracting. The yellow orbits are chaos, the red are orbits being attracted to the period-three points. The light-blue are orbits of transient chaos that also converge to the period-three points. The dark-blue orbits are elliptic, hence represent almost periodic solutions of the ODE. Near the small yellow orbits we find chaotic, almost-periodic, and transient-chaotic solutions coexisting.

5.6. Summary of nonlinear effects

In this section we have given five examples to illustrate four ways that nonlinearities may arise in autonomous two-dimensional ODEs: (1) nonlinear frequencies along linear orbits; (2) nonlinear relationship between linear orbits; (3) nonlinear divergence along linear orbits; (4) nonlinear or-

bits. These *nonlinear effects* may be combined as seen in Examples 4 and 5 to increase the level of complexity of an orbit. These effects present a different approach to autonomous systems than that provided by an analysis of its fixed points (Poincaré–Bendixon theory) because the nature of these effects contribute directly to the development of a level of complexity in nonlinear nonautonomous equations such as the Duffing equation. As shown in [Brown, 1992], any of these autonomous systems may be used in a construction that leads to autonomous three-dimensional equations that is the analog of the two-phase gate method. In this way, it is possible to construct ever increasingly complex examples of autonomous or nonautonomous systems with any predetermined level of complexity. The practical aspect of this lies in the applications of chaos to diverse areas of the mathematical and life sciences. The theoretical importance lies in the fact that the development of a theory of levels of complexity will have as its foundation a rich set of examples and counterexamples that can be used to guide the formulation and proof of the mathematical and physical theories.

6. Relationships Between Attractors, Noninvertibility, and Nondissipative Maps

Preliminary to this section we present some comments on dissipation, noninvertibility, and nonorientation-preserving properties of dynamical systems and their relationship to chaos.

6.1. Chaos and attractors

Many scientists associate chaos only with strange attractors or dissipative systems. For example, the Lorenz, Chua and Rossler equations are all dissipative. Historically, however, chaos was first mentioned⁵ as a nondissipative system. Chaos and attractors are independent concepts, and the most complex forms of chaos occur in nondissipative systems. In fact, the presence of dissipation reduces the level of complexity and thus reduces the “level” of chaos.

6.2. Chaos and noninvertibility

Noninvertible systems are inherently more complex than invertible systems. This is best illustrated by the fact that noninvertibility is a sufficient condition for a system to have positive entropy. Noninvertible systems do not directly arise from solutions of differential equations. This suggests that noninvertibility is a source of a level of complexity.

6.3. Nonorientation preserving and chaos

Orientation-preserving maps are those for which the Jacobian determinant is positive. The significance of this is that nonorientation-preserving maps cannot arise from the solutions of differential equations whose Jacobian is positive. There are many chaotic maps which are not orientation preserving; most notably, there are parameter values for which the Jacobian derivative of the Hénon map is negative. Hence, nonorientation-preserving maps are a source of some level of complexity. In this section we clarify some important relationships between dynamical systems having these three properties to give a perspective of how they contribute to the development of a level of complexity and to remove any confusion about their contribution to the production of chaos.

We summarize the relationships in a series of informal statements which can be rigorously proven.

Statement 1.

Any dissipative system that arises from an ODE can be converted to a nondissipative system without altering the fundamental level of complexity. Specifically, for any dissipative system we may increase the dimension of the system by one and make it, essentially, nondissipative. The construction is simple. Let $T(\mathbf{X})$ be any n -dimensional dissipative system. Since it arises from an ODE, the Jacobian determinant, $\det(DT(\mathbf{X}))$, must be positive. The following mapping “contains” T in an obvious sense and is nondissipative:

$$\begin{pmatrix} \mathbf{X} \\ z \end{pmatrix} \rightarrow \begin{pmatrix} T(\mathbf{X}) \\ z/(\det(DT(\mathbf{X}))) \end{pmatrix}. \quad (81)$$

This map expands in the direction of the added coordinate z by exactly the amount needed to keep the combined map nondissipative. Also, in this map T remains “intact.” The Jacobian determinant of the combined map is 1.

Statement 2.

Any noninvertible mapping can be made essentially invertible by doubling the number of coordinates. This was proven in [Brown & Chua, 1996b, Theorem 1] and is restated here for completeness.

Statement 3.

Any nondissipative map can be made dissipative in such a way that the original map is an attractor. Theorem 1 mentioned above also proves this statement.

Statement 4.

Any nonorientation-preserving mapping can be made orientation-preserving by increasing the dimension by one. A simplification of the construction of Statement 1 will do this: Add the coordinate $z \rightarrow -z$.

Statement 5.

Any mapping that can be written as a formula can be made the Poincaré map for some ODE for

⁵Poincaré in volume three, item 397, of his memoirs in reference to the level of complexity of the three-body problem. Poincaré never used the term *chaos* which was coined by Jim Yorke at the University of Maryland.

which an electronic circuit can be built. This result is a consequence of the above statements and the n -phase gate construction in [Brown & Chua, 1993]. As a result, we now expand Statement 1 as follows:

Statement 6.

Any dissipative system that can be written as a formula, regardless of whether it arises from an ODE, can be converted to a nondissipative system that does arise from an ODE without altering its level of complexity.

7. Summary

In this tutorial we have illustrated that there are degrees of chaos and that there are very interesting maps which are not considered chaotic but are more complex than much of what we call *chaos*. We conclude that it is impossible to talk of chaos in a meaningful way without also talking about the level of complexity of the chaotic system. From a practical point of view, there are nonchaotic systems that are just as useful in producing a high level of complexity as are many chaotic systems. Their use in spread-spectrum communications is a good practical example. Low-level encryption systems which are also low cost are another example. However, our philosophical wanderings have led us to suggest that there is a *theory of chaos* and that this theory is concerned with determining the ways in which complex outputs can arise from the action of dynamical systems, and with quantifying this level of complexity in a useful manner.

We have shown how nonlinearities can be formed in a variety of ways. The significance of this is that an application needing chaotic effects will be optimal if the construction assures that the chaos arises from the right processes. There are at least four different nonlinear processes in two dimensions that can be used to generate chaotic effects which have very different properties.

We have also shown that the features of dissipation, noninvertibility, and orientation-preserving are completely independent of chaos and can be added or subtracted from any application, as desired.

This paper is the fourth in a series of papers whose purpose is to clarify a wide range of issues about chaos through the construction of examples and counterexamples, [Brown & Chua, 1996a,

1996b, 1997] are the other three. In [Brown & Chua, 1996a] we presented 29 examples that answered such questions as “Can chaotic dynamical systems be solved in closed form in terms of elementary functions?”, “Does sensitive dependence on initial conditions ever define chaos?”, “What is the relationship between popular definitions of chaos?”, and several other questions. In [Brown & Chua, 1996b] we presented 26 examples that illustrated the spectrum of complexity that lies between Bernoulli chaos and periodic dynamics. In [Brown & Chua, 1997] we presented 6 examples to show that even the existence of positive Lyapunov exponents is not equivalent to chaos, that the shift paradigm is inadequate to account for all the features of chaos, and that highly complex orbits can be generated by chaotic dynamics without requiring that the initial conditions have positive algorithmic complexity. In this paper we presented 24 examples that: illustrated how subtle levels of chaos can be generated by combining a wide range of nonchaotic systems with chaotic systems; illustrated parts of the complexity spectrum that resemble chaos; and, how subtle nonlinear effects in autonomous two-dimensional systems can contribute to the formation of chaos. In total, we have constructed over 85 examples of dynamical systems in terms of elementary functions for which electronic circuits can be made that illuminate various aspects of chaos and the complexity spectrum and refute many popular notions about chaos. What we can conclude is that defining chaos is every bit as difficult as predicting chaos. Our examples suggest we conclude this paper with the following interesting line of thought.

Let us conceive of a n -dimensional space where one coordinate is entropy, another coordinate is correlation dimension, another coordinate is the Lyapunov exponent, and another the autocorrelation at some fixed time, and so on until we have exhausted all measures of levels of complexity found in a dynamical system. For each dynamical system, let us make all these measurements and plot its place in this space. We ask the question: Do the chaotic dynamical systems form a connected set, a compact set, or perhaps do they form a fractal? In short, just what is the nature of this set?

Acknowledgment

This work of the first author was supported in part by ONR contract N00014-95-C-0153.

References

- Arnold, V. & Avez, A. [1989] *Ergodic Problems of Classical Mechanics* (Addison-Wesley, New York).
- Brown, R. & Chua, L. O. [1996a] “Clarifying chaos: Examples and counterexamples,” *Int. J. Bifurcation and Chaos* **6**(2), 219–249.
- Brown, R. & Chua, L. O. [1996b] “From almost periodic to chaotic: The fundamental map,” *Int. J. Bifurcation and Chaos* **6**(6), 1111–1125.
- Brown, R. & Chua, L. [1993] “Dynamical synthesis of Poincaré maps,” *Int. J. Bifurcation and Chaos* **3**(5), 1235–1267.
- Cornfeld, I., Fomin, S. & Sinai, Y. [1982] *Ergodic Theory* (Springer-Verlag, Berlin).
- Ding, M., Grebogi, C. & Ott, E. [1989] “Evolution of attractors in quasiperiodically-forced systems: From quasiperiodic to strange nonchaotic to chaotic,” *Phys. Rev. A*, 2593–2598.
- Freeman, W. J. [1995] *Societies of Brains* (Lawrence Erlbaum Associates, Hillsdale, N.J).
- Grebogi, C., Ott, E., Pelikan, S. & Yorke, J. [1984] “Strange attractors that are not chaotic,” *Physica* **D13**, 261–268.
- Katznelson, Y. [1971] “Ergodic automorphisms of T^n are Bernoulli shifts,” *Israel J. Math.* **10**, 186–195.
- Parry, W. [1981] *Topics in Ergodic Theory* (Cambridge University Press, Cambridge).
- Peterson, K. [1983] *Ergodic Theory* (Cambridge University Press, Cambridge).
- Walters, P. [1982] *Introduction to Ergodic Theory* (Springer-Verlag, New York).